PROPAGATION OF PREMIXED FLAMES IN CONFINED CHANNELS

BY

ARJUN NAVANEETHA

THESIS

Submitted in partial fulfillment of the requirements
for the degree of Master of Science in Mechanical Engineering
in the Graduate College of the
University of Illinois at Urbana-Champaign, 2013

Urbana, Illinois

Adviser:

Professor Moshe Matalon

Abstract

The propagation of premixed flames in confined channels is investigated. In the unconfined case, the structure of the flame and the flame speed for the adiabatic planar flame have been numerically obtained and confirmed with the existing theory. It is seen that in the unconfined case, the flame propagates in nearly isobaric conditions with a constant flame speed whereas in the confined case there is pressure buildup which affects the flame speed. In the confined case, the time evolution of the flame is solved to obtain properties like the mass burning rate, pressure and flame location as a function of time, velocity field in the channel and propagation speed. Also the temperature and concentration profiles are obtained which give an insight in to the thickness of the flame region as the flame propagates through the entire channel. Effect of the Lewis number on the time taken for the flame to propagate the channel is examined. A non-linear analytical model that treats the flame as a discontinuity is also used to compare with the obtained numerical solution. This model requires only solving the hydrodynamic equations along with the Hugoniot jump relations across the flame front. The main difference between the numerical and the analytical solution is that the numerical solution takes into consideration a finite rate chemistry whereas in the analytical solution the reaction rate modeled as a delta function. Differences between the analytical and the numerical solution are compared.

To my family ...

Acknowledgments

This project would not have been possible without the support of many people. I would like to thank my adviser, Professor Moshe Matalon who was always there to guide and support me throughout the project. I would like to thank Navin Fogla, my friend and colleague for his tremendous support and valuable advice throughout this project. I would also like to thank Zhanbin Lu and Advitya Patyal who were always there to encourage and support me. I am also deeply indebted to the Mechanical Engineering and the Computer Science department at UIUC for providing me support in the form of assistantships.

Table of Contents

List of Figures

Chapter 1

Introduction

The propagation of premixed flames in confined channels has been a problem of great interest owing to their applications in diverse devices such as gas turbines for power generation and IC engines in automobiles. They also provide a deep insight into the interaction of the flame with the flow field. In the case of premixed flames in unconfined vessels, the flame freely propagates at a constant speed with no pressure build-up. The confined case is different from the unconfined one in the sense that there is a continuous build up of pressure and temperature. Also properties like the flame speed, mass burning rate are functions of the flame position and time.

Combustion in general involves several processes like heat transfer, mass transfer, chemical reactions that happen simultaneously over multiple temporal and spatial scales. The spatial scales include the flame thickness and the length of the channel within which combustion occurs. The reaction zone is a very thin region of the same order or smaller than the flame thickness, whereas the flame propagates through the entire channel whose length is a measure of the hydrodynamic scale making it imperative to consider both the length scales in our problem. Resolving such a multi-scale problem numerically requires in general a lot of computational resources which makes it difficult and expensive. By making appropriate assumptions, theoretical models have been developed which make use of the disparate nature of scales and through asymptotic analysis, lead to simplified problems which help in understanding the underlying physics of the problem.

The present analysis includes a combination of numerical and analytical techniques to describe the propagation of premixed flames in confined channels. In the case of unconfined

channels, one of the earliest asymptotic theories was suggested by Bush and Fendell [1, 2] in which the structure of a steady 1-D isobaric deflagration is studied for a one step chemical reaction. They also discussed a two-term asymptotic expression for the eigenvalue problem and obtained the laminar propagation speed for Lewis numbers of order unity with large activation energies. Following their work there has been a large number of studies that have exploited the largeness of the activation energy to understand flame behavior [3, 4, 5]. Exploring the multi-scale nature of the problem, Matalon and Matkowsky [6] treated the flame as a density discontinuity and through rigorous asymptotics, examined its propagation into an arbitrary flow that varies over distances comparable to the channel's length. They obtained an expression for the flame speed which depends upon the local curvature of the flame sheet and the hydrodynamic strain experienced by the flame. Cui et al. [7] obtained asymptotic expressions for the burning rate and flame shape by imposing a Poiseuille flow in a channel. They showed that the mass burning rate has a strong dependence on the Lewis number in the case of wide channels. Benkhaldoun, Larrouturou and Denet [8] performed 2-D numerical simulations for propagation of premixed curved flames in a tube with heat losses and also examined premixed flame extinction limits due to the heat losses. Daou and Matalon [9] studied the effect of the flow field (Poiseuille flow) on the propagation of premixed flames in a channel for a constant density model with no heat losses and discussed the flashback conditions and the long-term evolution of an ignition kernel. They also examined the propagation of pre-mixed flames in 2-D channels by accounting for heat losses by conduction to the channel walls assuming a Poiseuille flow in [10]. The problem of a flame propagating in long unconfined channels for a one step second order chemical reaction has been numerically studied by Kurdyumov and Matalon [11]. They examined the structure of the planar flame and also evaluated properties like pressure correction in the channel, the flow field and the time taken by the flame to propagate through the entire channel of given length.

In the case of premixed flames in confined channels, the pressure build up in the tube causes the temperature to rise continuously and its evolution in time has been studied by

various authors. Bradley and Mitcheson [12] presented a simple numerical model to evaluate the pressure in the closed vessel as a function of time. They have also studied the influence of temperature and pressure change with time on the burning velocity. Sivashinsky [13] proposed a hydrodynamic model of slow flame propagation in an enclosed volume including transport effects and chemical kinetics. Kooker [14, 15] solved the compressible Navier Stokes equation and developed a model for ignition and propagation of premixed flame in a confined chamber. The solution accounts for multi-species diffusion, finite rate chemical reactions and is restricted to ozone/oxygen mixtures. Fink, Fendell and Bush [16] numerically examined a 1-D premixed flame propagating into an enclosure whose volume was kept constant by varying the right wall boundary condition similar to what is actually experienced in SI engines. They have also taken non-adiabatic walls into consideration. Mcgreevy and Matalon [17] studied the effect of Lewis number on the propagation of premixed flames in confined channels. It was based on the hydrodynamic model similar to the one proposed by Sivashinsky [13]. Quantities such as temperature and flow fields on either side of the flame discontinuity, instantaneous location of the flame, the time taken by the flame to propagate through the channel have been calculated. They have also discussed the qualitatively different behaviors that occur with different Lewis numbers. Matalon and Metzener [18] discussed the stability of planar flames based on the Markstein parameter. A flat flame is obtained if the value of the Markstein parameter is greater than the critical Markstein parameter. Otherwise, the flame assumes cellular structure or a tulip shape. Also a non-linear evolution equation has been derived from the general conservation equations that describes the propagation of premixed flames in closed tubes. The formation and propagation of tulip flame structures is also discussed in [19, 20].

This thesis is organized as follows. In chapter 2, the non-dimensionalised form of the governing equations for a planar premixed flame are presented. In chapter 3, the structure of the flame and properties like the flame speed are obtained by solving the eigenvalue problem for a steady, unconfined flame. This solution is confirmed with the existing theory and the temperature, concentration profiles are used as an initial condition for the confined

case. In chapter 4, the problem of premixed flame in a confined channel is treated and two different methods used to analyze the problem are presented, namely the numerical solution and the analytical solution (Hydrodynamic model). In the case of the numerical solution, the ignition phase is not modeled and it is assumed that a steady planar flame under isobaric, adiabatic conditions has already been established a small distance away from the left boundary. The time evolution of this flame is studied and the findings are presented. The temperature field, concentration field, velocity fields have been shown. Also properties like the flame speed, propagation speed are calculated. This solution is further compared with the hydrodynamic solution which essentially treats the flame as an interface. This model requires solving the hydrodynamic equations along with the Hugoniot jump relations across the flame interface. The differences between these two solutions is that the numerical solution takes into consideration a finite rate chemistry whereas the hydrodynamic solution models the chemical reaction term as a delta function. In chapter 5, the differences in mass burning rate vs time and the flame location for these two methods are presented. For simplicity we ignore gravitational effects and heat losses in this discussion.

Chapter 2

Formulation

2.1 General form of the governing equations

The following work studies the propagation of a flame in a long channel of length l. The channel consists of a pre-mixed mixture of fuel and oxidizer which is ignited at the left end of the channel. A flame is considered to be established at the left boundary of the channel at time $t = 0$ and propagate to the right leaving hot products behind. In the following analysis, the chemistry is represented by a global one step reaction given by

$$Fuel + \nu\, Oxidizer \quad \rightarrow \quad Products,$$

where ν is the stoichiometric ratio of the reaction.

The mixture is assumed to be lean in fuel and the mass fraction of the oxidizer remains nearly constant. It is therefore sufficient to follow the evolution of the fuel only, with mass fraction Y. The walls are assumed to be adiabatic, that is no heat transfer can take place across it.

2.1.1 Subscripts used in this discussion

0 reference state at an initial time

e reference state at the ending time when the flame is at the end of the channel.

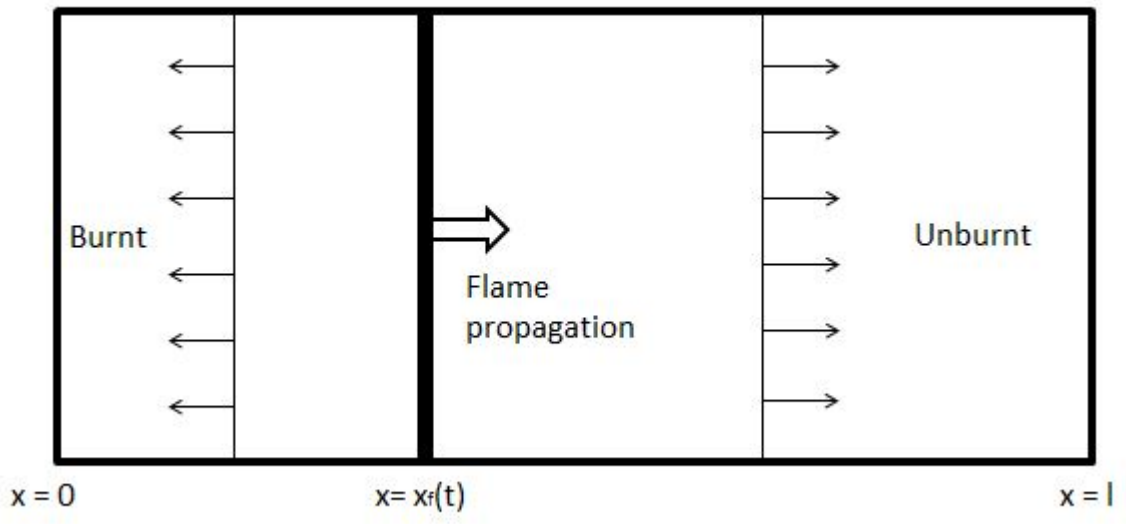

Figure 2.1: Propagation of a flame front in a channel closed at both ends

2.1.2 Nomenclature

l length of tube

t time

p dynamic pressure

ρ density

T temperature

P mean pressure level in the tube

$\vec{v}$ velocity

Ma Mach number

M mass burning rate

R universal gas constant

c_p mixture specific heat at constant pressure

c_v mixture specific heat at constant volume

γ c_p/c_v

λ mixture thermal conductivity

W mean molecular weight of the mixture

B pre-exponential factor

Y reactant (fuel) mass fraction

E activation energy

Q heat of combustion per unit mass of the reactant

V volume of the tube

V_f normal velocity of the front

$\mathcal{D}$ binary diffusivity of the defined reactant (fuel) into the bulk

2.1.3 General form of the governing equations

For simplicity, we have assumed equal specific heats and molecular weights for all species and that the molecular weight of the mixture W, viscosity coefficient μ, thermal conductivity λ and diffusion coefficient $\rho\mathcal{D}$ are all constants.

The mass conservation equation is

$$\frac{D\rho}{Dt} + \rho\nabla \cdot \vec{v} = 0.$$

The momentum equation is

$$\rho\frac{D\vec{v}}{Dt} = -\nabla p + \mu(\nabla^2\vec{v} + \frac{1}{3}\nabla(\nabla \cdot \vec{v})).$$

The energy conservation equation is

$$\rho c_p\frac{DT}{Dt} - \lambda\nabla^2 T = \frac{Dp}{Dt} + QB\frac{\rho Y}{W}e^{-E/RT}.$$

The equation for the concentration of species is given as

$$\rho\frac{DY}{Dt} - \rho\mathcal{D}\nabla^2 Y = -B\frac{\rho Y}{W}e^{-E/RT}.$$

The equation of state is

$$P = \frac{\rho RT}{W}.$$

2.2 Non-dimensionalization form of the governing equations

2.2.1 Non-dimensionalization parameters

The parameters used to non-dimensionalize the general form of the equations are described below ($*$ denotes dimensionless quantities):

$$x^* = \frac{x}{l_f}\ ,\ \rho^* = \frac{\rho}{\rho_0}\ ,\ p^* = \frac{p}{P_0},\ T^* = \frac{T}{T_0},\ Y^* = \frac{Y}{Y_0},\ L^* = \frac{l}{l_f},\ u^* = \frac{u}{S_L} \text{ and } t^* = \frac{S_L t}{l_f}.$$

In the non-dimensionalization parameters mentioned above, x is the longitudinal coordinate, u is the velocity component in the x direction. ρ_0 is the density of the fresh mixture, $l_f = D_{th}/S_L$ is the flame thickness, $D_{th} = \lambda/\rho_u c_p$ is the thermal diffusivity of the mixture where c_p is the specific heat at constant pressure of the mixture, Y_0 is the mass fraction of fuel in the fresh mixture, P_0 is the initial pressure in the channel (e.g. equal to the atmospheric pressure), T_0 is the temperature of the fresh mixture and S_L is the laminar flame speed (under isobaric, adiabatic conditions).

The adiabatic flame temperature T_a and laminar flame speed S_L are properties of the given mixture. Under the adopted simplification, the adiabatic flame temperature takes the form

$$T_a = T_0 + \frac{QY_0}{c_p}, \tag{2.1}$$

but the flame speed S_L needs to be determined numerically. An approximation to S_L for

$\beta \to \infty$ is given by

$$(S_L)_{Asym} = \sqrt{\frac{2D_{th}B}{\sigma\beta^2 Le^{-1}}}\, e^{-E/2RT_a}. \tag{2.2}$$

2.2.2 Low Mach number approximation

The propagation speed of ordinary deflagration waves is in the range of 1-100 cm/s, which is much smaller than the speed of sound (in air c= 34000 cm/s). The representative Mach number is therefore very small ($Ma << 1$). The consequence of this assumption is that pressure (p) may be expressed as $p = P(t) + \gamma Ma^2\, p'(x,t) + ...$ The pressure in the channel is equalized instantaneously everywhere with small spatial correction (p') on the order of Ma^2 only. In an unconfined channel $P(t) = 1$, corresponding to the atmospheric pressure conditions. In the case of confined channels the mean pressure in the channel $P(t)$ varies with time.

2.2.3 Non-dimensionalized form of the governing equations in Cartesian coordinates

While describing the non-dimensionlized form of the equations from now onwards, we will represent all the terms without a star ($*$) for the sake of simplicity. We have also removed the prime ($'$) in the pressure correction term which appears in the momentum equation. The governing equations in the non-dimensional form in one dimension are as follows:

The mass conservation equation is

$$\frac{\partial \rho}{\partial t} + \frac{\partial}{\partial x}(\rho u) = 0. \tag{2.3}$$

The momentum conservation equation is

$$\rho\left(\frac{\partial u}{\partial t} + u\frac{\partial u}{\partial x}\right) = -\frac{\partial p}{\partial x} + \frac{4}{3}Pr\frac{\partial^2 u}{\partial x^2}. \tag{2.4}$$

The energy conservation equation is

$$\rho\left(\frac{\partial T}{\partial t}+u\frac{\partial T}{\partial x}\right)=\frac{\partial^2 T}{\partial x^2}+\left(\frac{\gamma-1}{\gamma}\right)\frac{dP}{dt}+q\omega. \tag{2.5}$$

The equation for the concentration of species is given as

$$\rho\left(\frac{\partial Y}{\partial t}+u\frac{\partial Y}{\partial x}\right)=\frac{1}{Le}\frac{\partial^2 Y}{\partial x^2}-\omega. \tag{2.6}$$

The equation of state is

$$P(t)=\rho T. \tag{2.7}$$

The reaction rate term ω is given by

$$\omega(T,Y)=\frac{\beta^2}{2s_L^2 Le}\rho Y e^{\beta T_a(T_a-1)/(T_a-1)T}.$$

Here the adiabatic flame temperature in non-dimensional form obtained from equation (2.1) is

$$T_a=1+q, \tag{2.8}$$

where q is the heat release parameter given by $\dfrac{QY_{F_0}}{c_pT_0}$ and β is the Zel'dovich number defined as $\beta=\dfrac{E(T_a-T_0)}{RT_a{}^2}$. The parameter s_L is the ratio of the laminar flame speed (S_L) to the flame speed in the asymptotic limit $(S_L)_{Asym}$,

$$s_L=\frac{S_L}{(S_L)_{Asym}}, \tag{2.9}$$

which has to be calculated numerically.

The Lewis number is defined as the ratio of the thermal diffusivity to the mass diffusivity, that is $Le=D_{th}/\mathcal{D}$. The Prandtl number is the ratio of the viscous to the thermal diffusivity of the mixture and defined as $Pr=\mu c_p/\lambda$.

Chapter 3

Unconfined planar flame

In this topic, we will be discussing the propagation of a planar premixed flame in an unconfined environment. The mean pressure in the channel equals the atmospheric pressure and in non-dimensional form is given by $P = 1$.

3.1 Constant density model

3.1.1 Governing equations for the constant density model

In this model, the density doesn't vary in space and time. The value of density in the non-dimensional form is $\rho = 1$ an equation that replaces the equation of state.

The continuity equation is

$$\frac{\partial u}{\partial x} = 0 \tag{3.1}$$

and in a frame attached to the flame, $u = 1$ everywhere in the channel.

The energy conservation equation is conveniently written as

$$\frac{\partial \theta}{\partial t} + \frac{\partial \theta}{\partial x} = \frac{\partial^2 \theta}{\partial x^2} + \omega, \tag{3.2}$$

where $\theta = \dfrac{T-1}{T_a - 1} = \dfrac{T-1}{q}$.

The equation for the concentration of species is given as

$$\frac{\partial Y}{\partial t} + \frac{\partial Y}{\partial x} = \frac{1}{Le}\frac{\partial^2 Y}{\partial x^2} - \omega, \tag{3.3}$$

where

$$\omega = \frac{\beta^2}{2s_L^2 Le} Y e^{\beta\sigma(\theta-1)/1+(\sigma-1)\theta},$$

The thermal expansion constant (σ) is defined as the ratio of the density of the unburnt gas to density of the burnt gas mixture.

$$\sigma = \frac{T_a}{T_u} = \frac{\rho_u}{\rho_b} \tag{3.4}$$

such that $\sigma > 1$. Note also that $\sigma = 1 + q$.

3.1.2 Boundary conditions

The boundary conditions are as follows:

At $x = -\infty$ (burnt state)

$$\theta = 1,$$

$$Y = 0,$$

$$\frac{\partial Y}{\partial x} = 0,$$

$$\frac{\partial \theta}{\partial x} = 0.$$

At $x = \infty$ (unburnt state)

$$\theta = 0,$$

$$Y = 1,$$

$$\frac{\partial Y}{\partial x} = 0,$$

$$\frac{\partial \theta}{\partial x} = 0.$$

Equations (3.1) - (3.4) and the BC's mentioned above constitute a problem that need to be solved subject to appropriate IC's. We are interested in numerically calculating the flame speed parameter s_L as the function of the Lewis number and the Zel'dovich number (β).

3.1.3 Numerical procedure and Results

The time-derivative term is set to 0 in the above equations and the governing equations are then solved to obtain a steady state solution. A boundary value problem solver BVP4C in MATLAB was used to solve the above system of ODE's and to determine the eigenvalue (flame speed parameter s_L) in the above problem.

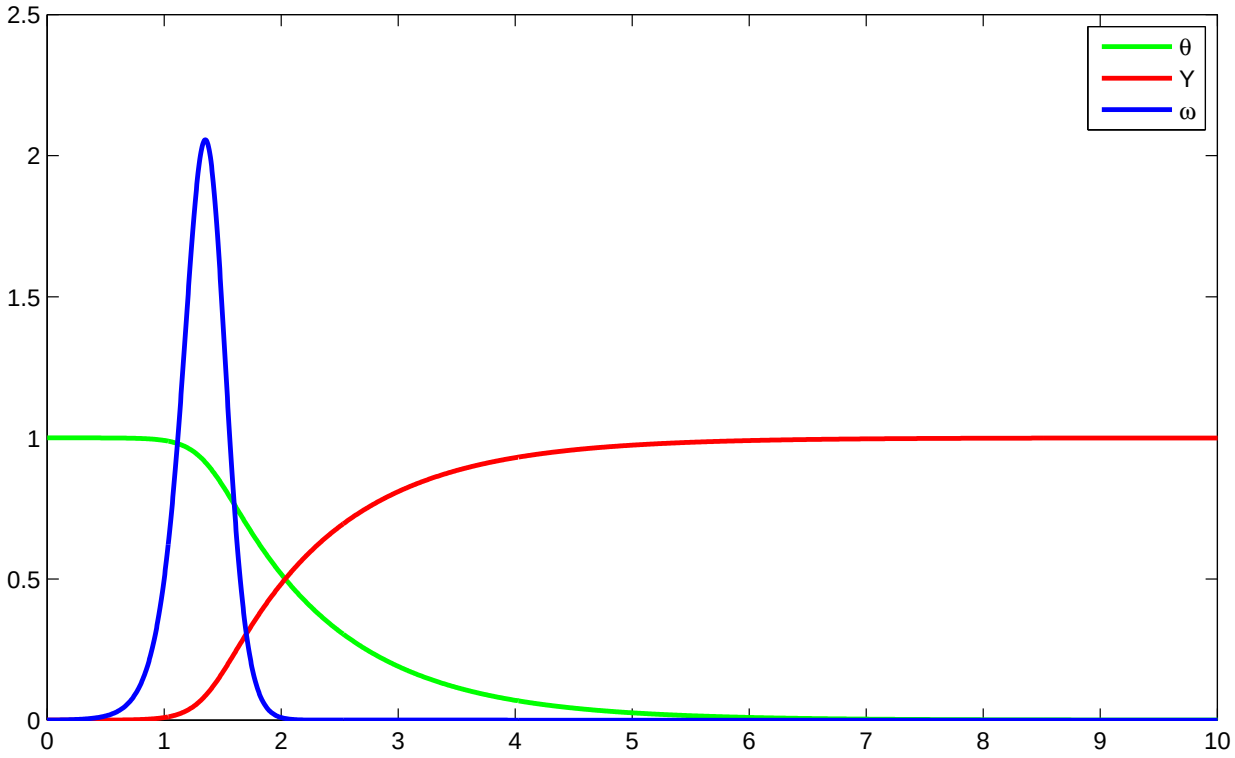

Figure 3.1: Profiles for θ, Y and ω obtained for $Le = 1$, $\sigma = 6-$ constant density model

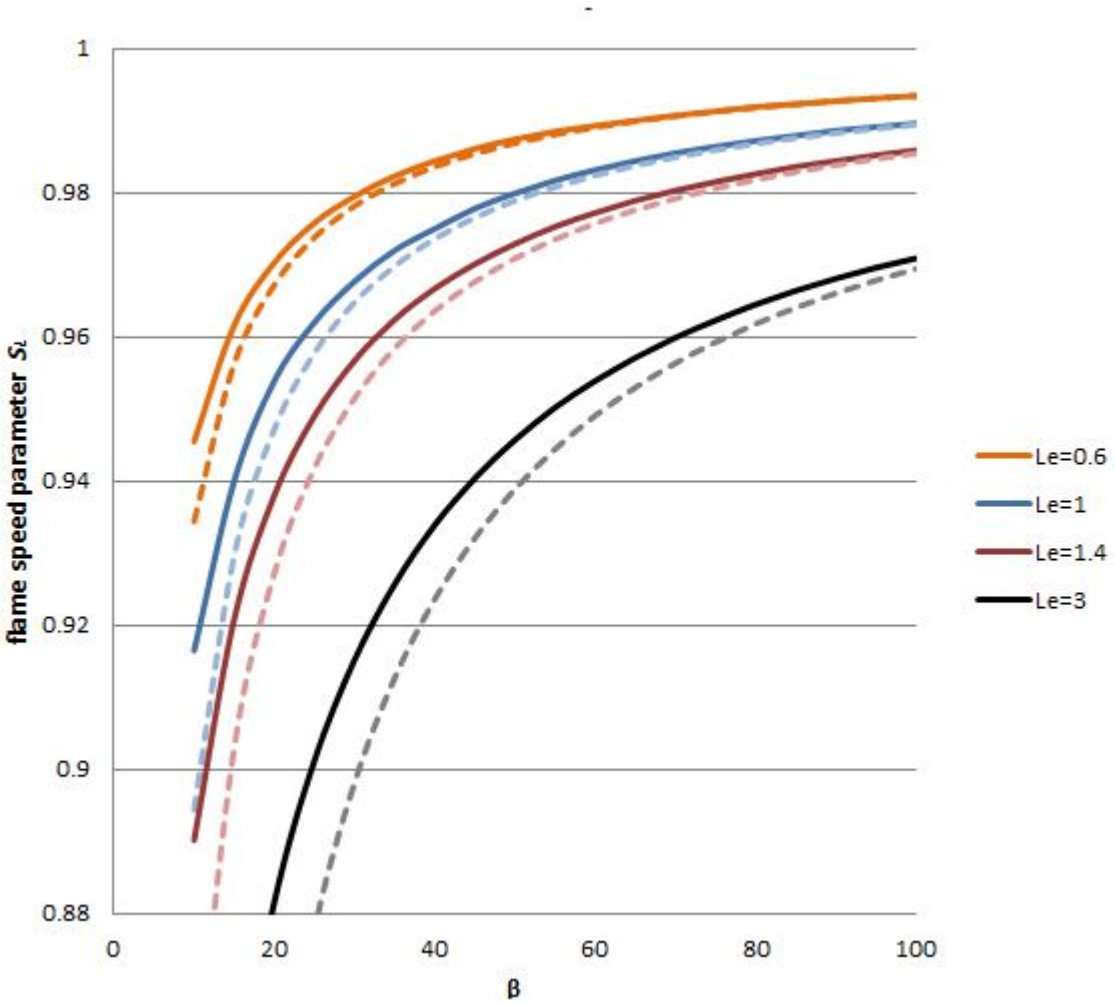

Figure 3.2: Comparison of the flame speed parameter s_L between the 2-term asymptotic result and the numerical solution : s_L vs. β plotted for $Le = 0.6, 1, 1.4, 3$ and $\sigma = 5$

In figure 3.1, the profiles obtained for the temperature, concentration and reaction rate are shown for a Lewis number of 1 . The Zel'dovich number (β) is taken to be equal to 10.

In the figure 3.2, different curves corresponding to different Lewis numbers are shown by different colors. For each of these Lewis numbers, the value of β was varied and the corresponding value of flame speed parameter s_L plotted on the y - axis. These correspond to the solid lines which, as noted were normalized wrt to the one term expression for $(S_L)_{Asym}$ given by equation 2.2 specifically

$$s_L = \frac{S_L}{(S_L)_{Asyms}}, \quad (S_L)_{Asym} = \sqrt{\frac{2D_{th}B}{\sigma\beta^2 Le^{-1}}}\, e^{-E/2RT_a}.$$

The broken curves are the two-term asymptotic result described in [1] for approximating the asymptotic flame speed $(S_L)_{Asym}$ in the limit of large activation energy [21, 5] which is given by:

$$(S_L)_{Asym} = \left[1 - \beta^{-1}\left(3\frac{\sigma-1}{\sigma} - (1-Le) - 1.344045\right)\right]\sqrt{\frac{2D_{th}B}{\sigma\beta^2 Le^{-1}}}\, e^{-E/2RT_a}. \tag{3.5}$$

It is seen that the two curves approach each other in the limit $\beta \to \infty$ and that the value of $s_L \to 1$ in this limit. These results have been presented for a value of $\sigma = 5$ in order to compare with the results shown in [21].

3.2 Variable density model

3.2.1 Governing equations for the variable density model

We now consider density variations. The governing equations are as follows:
The mass conservation equation is

$$\frac{\partial \rho}{\partial t} + \frac{\partial}{\partial x}(\rho u) = 0. \tag{3.6}$$

The energy conservation equation is

$$\rho\frac{\partial \theta}{\partial t} + \rho u\frac{\partial \theta}{\partial x} = \frac{\partial^2 \theta}{\partial x^2} + \omega. \tag{3.7}$$

The equation for the concentration of species is given as

$$\rho\frac{\partial Y}{\partial t} + \rho u\frac{\partial Y}{\partial x} = \frac{1}{Le}\frac{\partial^2 Y}{\partial x^2} - \omega. \tag{3.8}$$

The equation of state is

$$\rho = \frac{1}{1+(\sigma-1)\theta}, \tag{3.9}$$

where

$$\omega = \frac{\beta^2}{2s_L^2 Le}\left(\frac{\sigma}{1+(\sigma-1)\theta}\right) Y e^{\beta\sigma(\theta-1)/1+(\sigma-1)\theta}.$$

3.2.2 Boundary conditions, Numerical procedure

The boundary conditions remain the same as specified above. The steady state problem (by setting $\frac{\partial}{\partial t} = 0$ in equations (3.6) - (3.8) and using the equation of state equation (3.9)) is solved using a similar numerical procedure (Boundary value solver - BVP4C in MATLAB) as mentioned in the constant density model.

3.2.3 Plots and Results

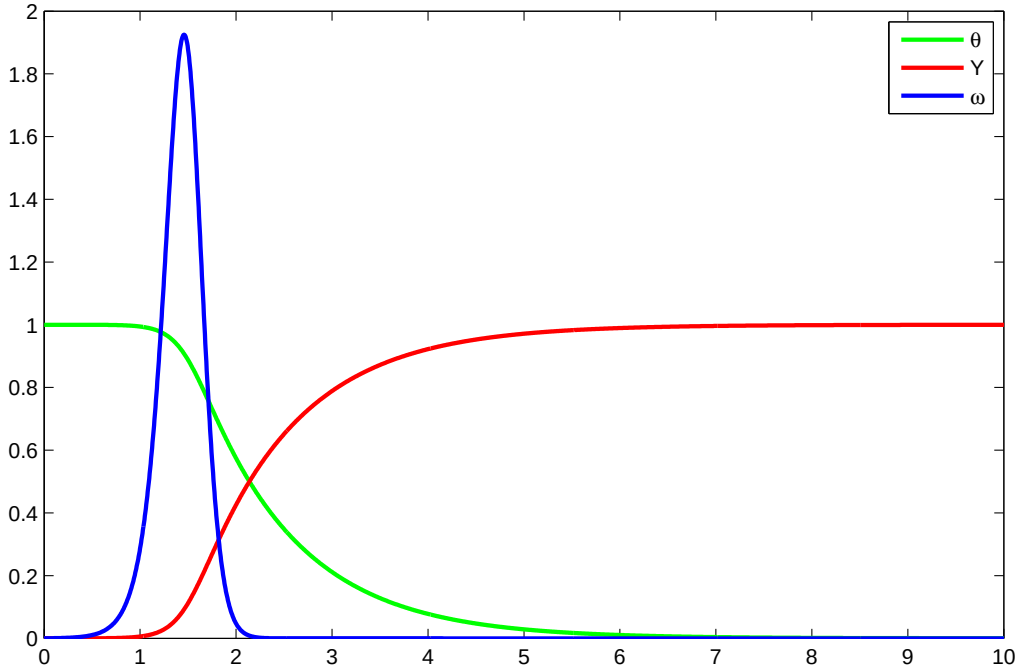

Figure 3.3: Profiles for θ, Y and ω obtained for $Le = 1$, $\sigma = 6-$ variable density model

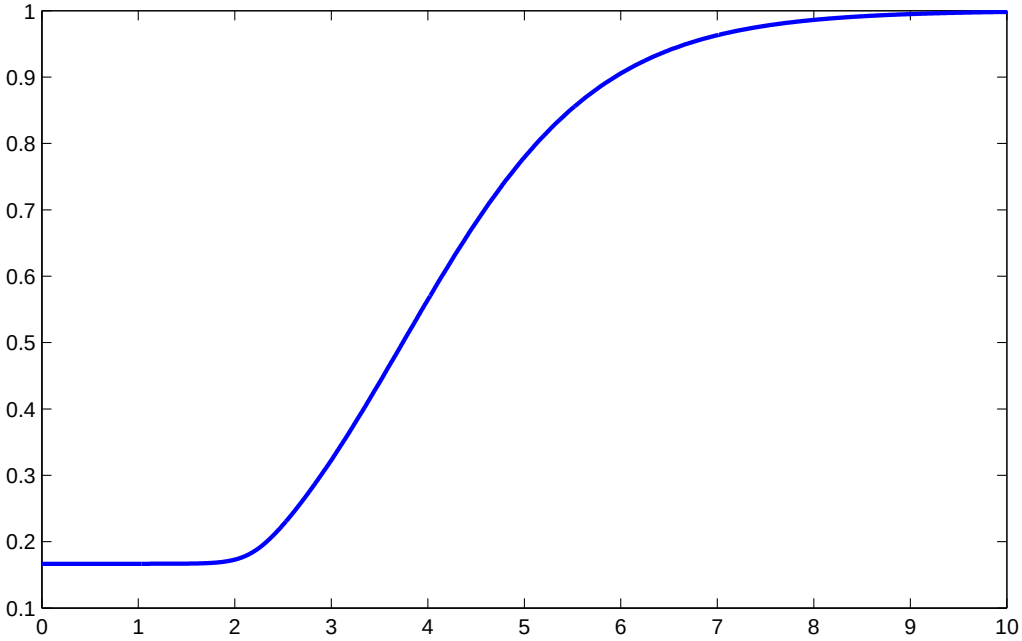

Figure 3.4: Density profile obtained for $Le = 1$ and $\sigma = 6$

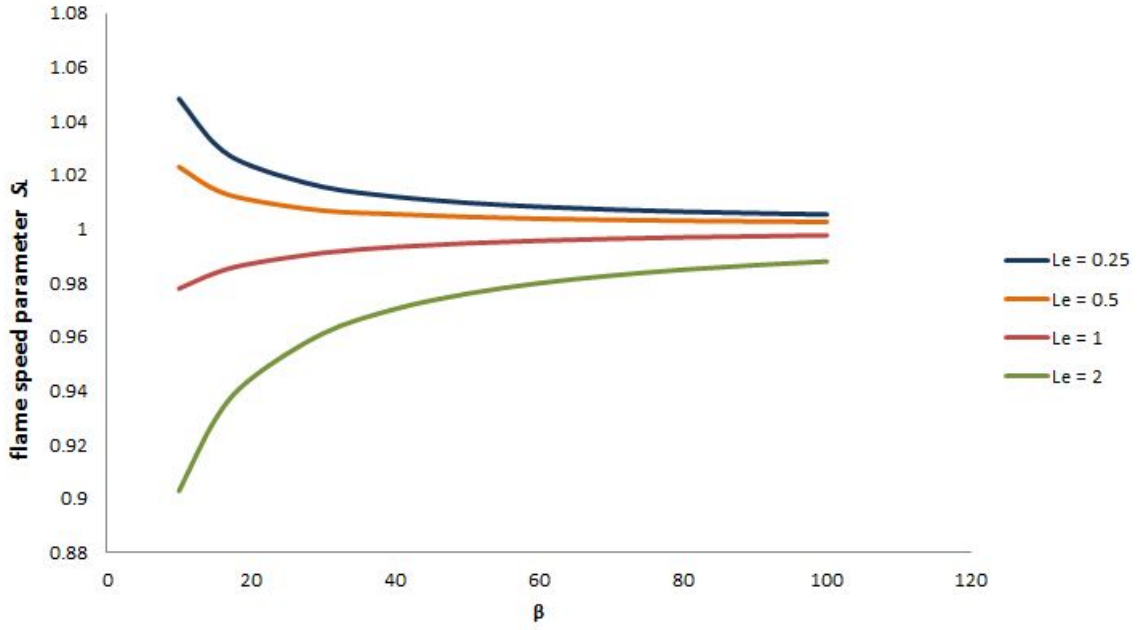

Figure 3.5: Flame speed parameter s_L defined in equation (2.9) vs. β plotted for $Le = 0.6, 1, 1.4, 3$ and $\sigma = 6$

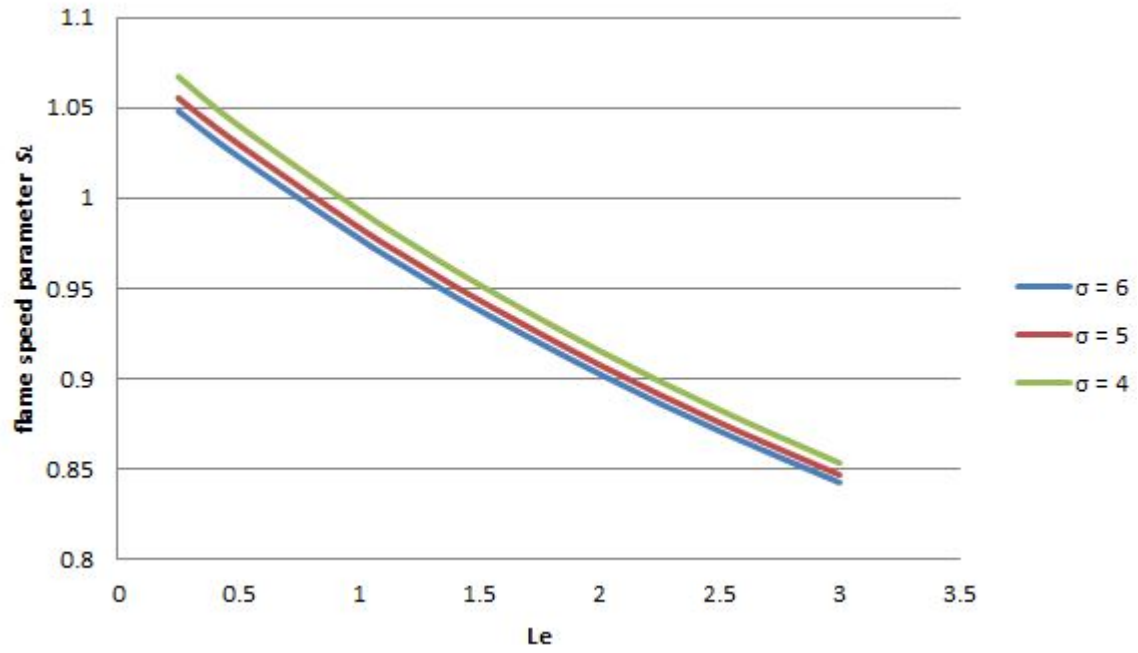

Figure 3.6: Flame speed parameter s_L defined in equation (2.9) vs. Le plotted for $\sigma = 4, 5, 6$

The profiles of temperature, concentration and reaction rate are plotted in figure 3.3 for $Le = 1$, Zel'dovich number (β) of 10 and the ratio of unburnt to burnt density ratio (σ) of 6. Figure 3.4 is the density profile shown for the same parameters. In figure 3.5, s_L is plotted as a function of β for different values of the Lewis numbers, but the unburnt to burnt density ratio is fixed ($\sigma = 6$). As the Zel'dovich number becomes higher, the value of s_L approaches 1 as shown in the figure. In figure 3.6, s_L is plotted with Lewis number for different values of the unburnt to burnt density ratios and are plotted for a fixed value of the Zel'dovich number (β=10).

3.2.4 Steadily propagating flame

A steadily propagating flame can be obtained using the calculated value of flame speed parameter s_L from above. To obtain this, an additional expression for the velocity field is used which is derived as mentioned below.

Multiplying the mass conservation equation (3.6) by $(1 + (\sigma - 1)\theta)$, we get

$$\Big(1 + (\sigma - 1)\theta\Big)\frac{\partial \rho}{\partial t} + \Big(1 + (\sigma - 1)\theta\Big)\frac{\partial}{\partial x}(\rho u) = 0.$$

By multiplying the energy equation (3.7) by $(\sigma - 1)$, we get

$$(\sigma - 1)\rho\frac{\partial \theta}{\partial t} + (\sigma - 1)\rho u\frac{\partial \theta}{\partial x} = (\sigma - 1)\frac{\partial^2 \theta}{\partial x^2} + (\sigma - 1)\omega.$$

Adding these two expressions together, we get

$$\frac{\partial\Big(\rho(1 + (\sigma - 1)\theta)\Big)}{\partial t} + \frac{\partial}{\partial x}\Big(\rho u(1 + (\sigma - 1)\theta)\Big) = (\sigma - 1)\frac{\partial^2 \theta}{\partial x^2} + (\sigma - 1)\omega.$$

Using the equation of state (3.9) we have,

$$\frac{\partial u}{\partial x} = (\sigma - 1)\frac{\partial^2 \theta}{\partial x^2} + (\sigma - 1)\omega.$$

This expression is further integrated to get the velocity field by using the conditions that the unburnt gas far to the right end is at rest, giving

$$u(x,t) = (\sigma - 1)\frac{\partial \theta}{\partial x}\bigg|_x - (\sigma - 1)\int_x^{\infty} (\omega dx), \tag{3.10}$$

where $-\infty < x < \infty$.

In the previous subsection, the plots are obtained for the steady state problem where the flame is maintained stationary via a constant unburnt gas velocity. A steadily propagating flame can also be obtained where the unburnt gas is stationary and the flame moves from left to right. The time evolution problem consisting of equations ((3.6) - (3.9) and (3.10)) are solved by using a 4^{th} order spatial discretization scheme and a time marching Adams Bashforth method. Figure 3.8 is an example of the temperature profile of a steadily propagating flame in an unconfined environment. Figure 3.9 shows the concentration profile of the steadily propagating flame. If the location of flame vs time is plotted, the slope is obtained to be equal to 1 as in figure 3.7 which means that the non-dimensional flame speed is equal to 1.

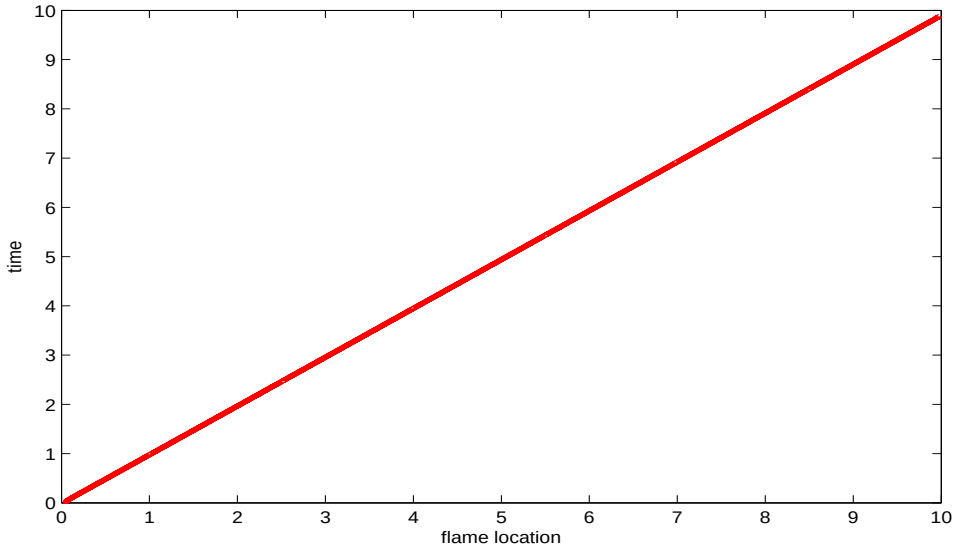

Figure 3.7: Flame location vs time of a steadily propagating planar unconfined flame

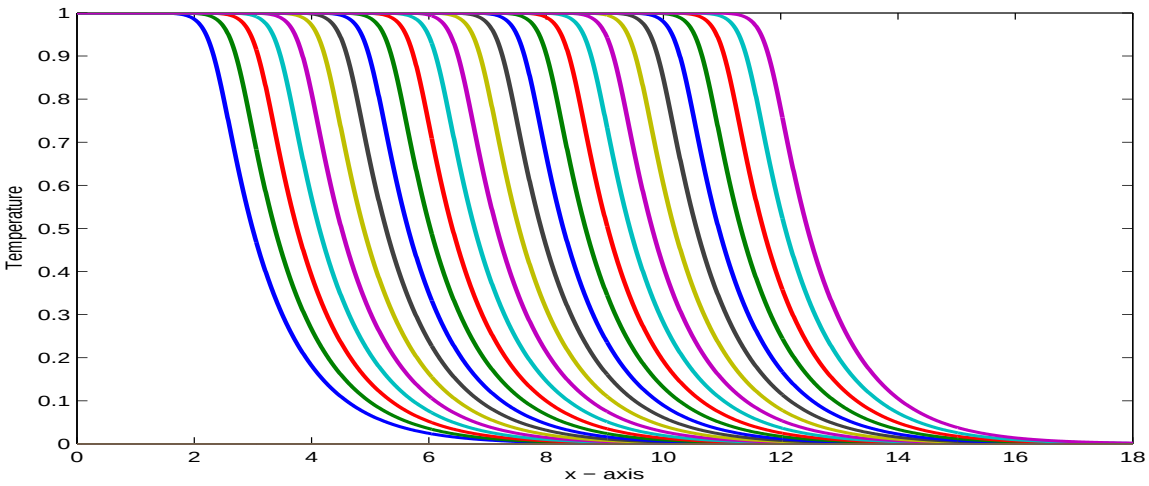

Figure 3.8: Temperature profile of a steadily propagating planar unconfined flame

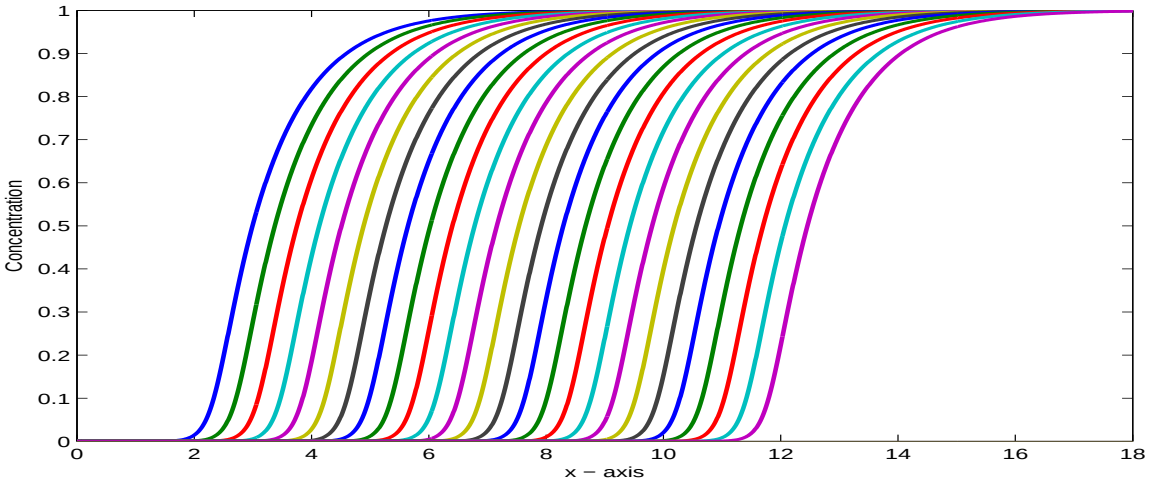

Figure 3.9: Concentration profile of a steadily propagating planar unconfined flame

Chapter 4

Confined planar flame

In this topic, we will be discussing the propagation of premixed flames in a confined channel of length L where $L = \frac{l}{l_f}$, L is the non-dimensionalized length of the channel. Two different models to solve the problem of propagation of premixed flames in a confined channel are discussed below. The first model is a numerical solution to the full form of the governing equations with finite rate chemistry. The second model is the hydrodynamic model - an analytical solution to the governing equations by making the simplifying approximation of a thin flame with a reaction rate approximated by a delta-function.

4.1 Flame propagation in a confined channel - Numerical solution

4.1.1 Governing equations for the numerical model

The governing equations are solved here numerically. The equations are:
The mass conservation equation is :

$$\frac{\partial \rho}{\partial t} + \frac{\partial}{\partial x}(\rho u) = 0.$$

The energy conservation equation is

$$\rho \frac{\partial T}{\partial t} + \rho u \frac{\partial T}{\partial x} = \frac{\partial^2 T}{\partial x^2} + \left(\frac{\gamma - 1}{\gamma}\right) \frac{dP}{dt} + q\omega.$$

The equation for the concentration of species is given as

$$\rho\frac{\partial Y}{\partial t}+\rho u\frac{\partial Y}{\partial x}=\frac{1}{Le}\frac{\partial^2 Y}{\partial x^2}-\omega.$$

The equation of state is

$$P(t)=\rho T.$$

4.1.2 Boundary conditions and expression for the velocity field

The boundary conditions are as follows:

At $x=0$ and $x=L$

$$\frac{\partial Y}{\partial x}=0,$$

$$\frac{\partial \theta}{\partial x}=0,$$

$$u=0.$$

An expression for the velocity field can be obtained as obtained as follows. Multiplying the mass conservation equation by T, then adding it to the energy conservation equation and using the equation of state we get ,

$$\frac{\partial u}{\partial x}=\frac{1}{P}\left(\frac{-1}{\gamma}\frac{dP}{dt}+\frac{\partial^2 T}{\partial x^2}+q\omega\right).$$

If the above equation is integrated w.r.t x and after applying the boundary condition for u at $x=L$, an expression for the velocity field is obtained as

$$u(x,t)=\frac{1}{P}\left(\frac{1}{\gamma}\frac{dP}{dt}(L-x)+\frac{\partial T}{\partial x}-q\int_x^L(\omega dx)\right). \tag{4.1}$$

The reaction rate is given as

$$\omega(T,Y)=\frac{\beta^2}{2s_L^2 Le}\rho Y e^{\beta T_a(T_a-1)/(T_a-1)T}.$$

An **equation for change in pressure with time** can be obtained by multiplying the mass conservation equation by T, and adding the energy conservation equation and further using the equation of state. This gives,

$$\frac{1}{\gamma}\frac{dP}{dt} + \frac{\partial}{\partial x}(Pu - \frac{\partial T}{\partial x}) = q\omega.$$

The above equation can be integrated w.r.t to x. Then by making use of the boundary conditions which are mentioned above, we get

$$\frac{dP}{dt} = \frac{\gamma q}{L}\int_0^L (\omega dx). \tag{4.2}$$

4.1.3 Numerical Procedure

In the above equations s_L is the known flame speed parameter which has been computed in the unconfined channel case - variable density model described in the previous chapter.

The numerical methodology used to solve the propagation of premixed flames in a confined

channel is explained here. The grid is divided into N equally spaced points and numbered as 1, 2.... $N-1$, N.

The 1^{st} order derivatives were calculated using a $4th$ order accurate spatial discretization scheme mentioned below.

For the 1^{st} node, the boundary condition is applied.

$$\left(\frac{\partial T}{\partial x}\right)_1 = 0$$

For the 2^{st} node,

$$\left(\frac{\partial T}{\partial x}\right)_2 = \frac{1}{12\Delta x}\left(-3T_1 - 10T_2 + 18T_3 - 6T_4 + T_5\right)$$

For the inner nodes from $i = 3$ to $N - 2$, central differencing spatial discretization scheme is used.

$$\left(\frac{\partial T}{\partial x}\right)_i = \frac{1}{12\Delta x}\left(-T_{i+2} + 8T_{i+1} - 8T_{i-1} + T_{i-2}\right)$$

For the 2^{nd} last node,

$$\left(\frac{\partial T}{\partial x}\right)_{N-1} = \frac{1}{12\Delta x}\left(3T_N + 10T_{N-1} - 18T_{N-2} + 6T_{N-3} - T_{N-4}\right)$$

For the last node, the boundary condition is applied.

$$\left(\frac{\partial T}{\partial x}\right)_N = 0$$

The 2^{nd} order derivatives were calculated using a $4th$ order accurate spatial discretization scheme mentioned below.

For the 1^{st} node, one-sided finite difference spatial discretization scheme is used.

$$\left(\frac{\partial^2 T}{\partial x^2}\right)_1 = \frac{1}{12\Delta x^2}(11T_5 - 56T_4 + 114T_3 - 104T_2 + 35T_1)$$

For the 2^{st} node,

$$\left(\frac{\partial^2 T}{\partial x^2}\right)_2 = \frac{1}{12\Delta x^2}(11T_1 - 20T_2 + 6T_3 + 4T_4 - T_5)$$

For the inner nodes from $i = 3$ to $N - 2$, central differencing spatial discretization scheme is used

$$\left(\frac{\partial^2 T}{\partial x^2}\right)_i = \frac{1}{12\Delta x^2}(-T_{i-2} + 16T_{i-1} - 30T_i + 16T_{i+1} - T_{i+2})$$

For the 2^{nd} last node,

$$\left(\frac{\partial^2 T}{\partial x^2}\right)_{N-1} = \frac{1}{12\Delta x^2}(11T_N - 20T_{N-1} + 6T_{N-2} + 4T_{N-3} - T_{N-4})$$

For the last node, one sided spatial discretization scheme is used.

$$\left(\frac{\partial^2 T}{\partial x^2}\right)_{N} = \frac{1}{12\Delta x^2}(11T_{N-4} - 56T_{N-3} + 114T_{N-2} - 104T_{N-1} + 35T_N)$$

The time integration is done using a three-step Adams Bashforth method where n denotes the current time instant.

$$T_{n+3} = T_{n+2} + \Delta t(\frac{23}{12}F(t_{n+2}, T_{n+2}) - \frac{4}{3}F(t_{n+1}, T_{n+1}) + \frac{5}{12}F(t_n, T_n)).$$

In this model, the value of $\Delta x = 0.008$. The value of $\Delta t = 10^{-6}$. Also since the region of interest is very very small compared to the actual size of the actual domain, it was necessary to use a non-uniform grid. Hence it was necessary to use the technique of Adaptive Mesh Refinement (AMR) which helped in reducing the time it took for the actual simulation to run. As the flame propagates from left to right , the entire mesh is modified with time, so that the fine portion of the mesh is always in the region where the reaction zone is located. With the AMR, the smallest value of $\Delta x = 0.004$ in the region of the flame and the largest value of $\Delta x = 0.01$. The value of $\Delta t = 10^{-6}$. It was also verified that by taking smaller values of Δx and Δt, the results obtained were almost identical.

In-order to find the location of the flame, a Taylor series expansion is used to evaluate the location of the flame from the grid point where the value of ω is maximum.

$$x_f = x_i - \frac{\left(\frac{\partial \omega}{\partial x}\right)_i}{\left(\frac{\partial^2 \omega}{\partial x^2}\right)_i},$$

where x_i indicates the location of the maximum value of ω. Once the value of x_f is computed, the propagation speed is calculated as the derivative of $\frac{\partial x_f}{\partial t}$.

4.1.4 Results and plots:

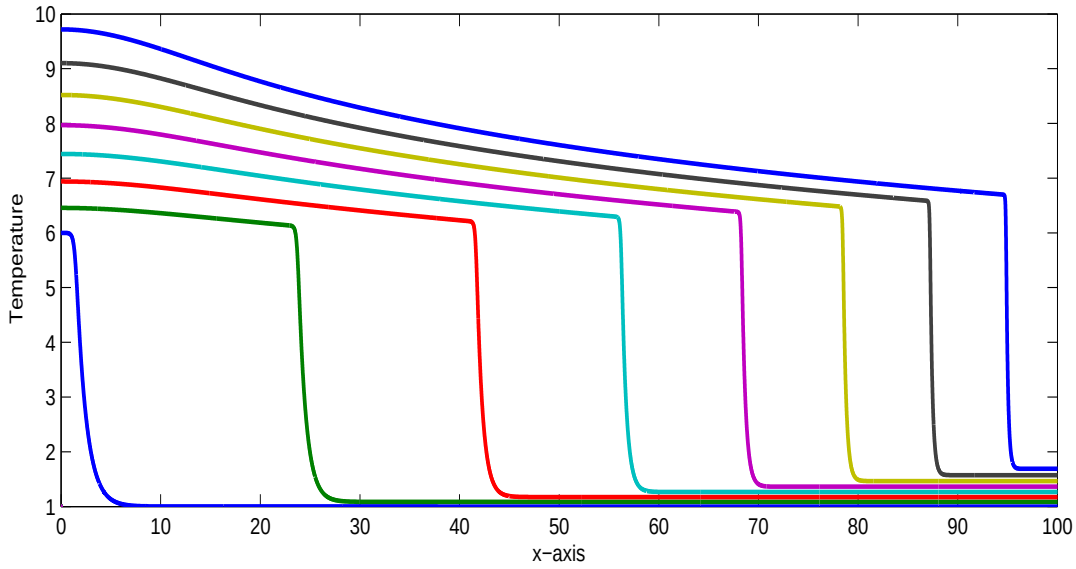

Figure 4.1: Temperature vs. $x - axis$ for $q = 5$ at consecutive time steps

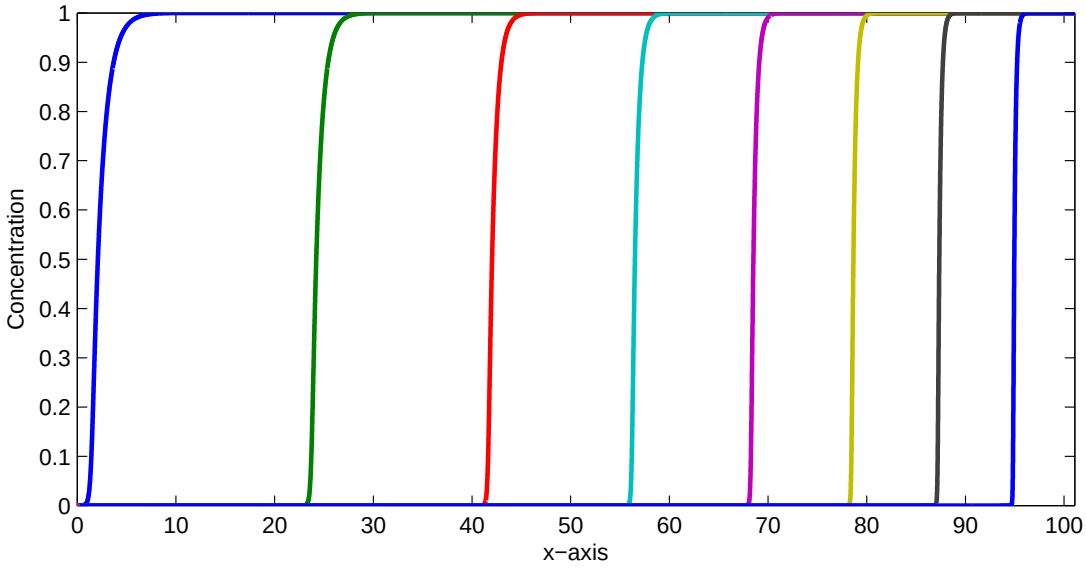

Figure 4.2: Concentration vs. $x - axis$ for $q = 5$ at consecutive time steps

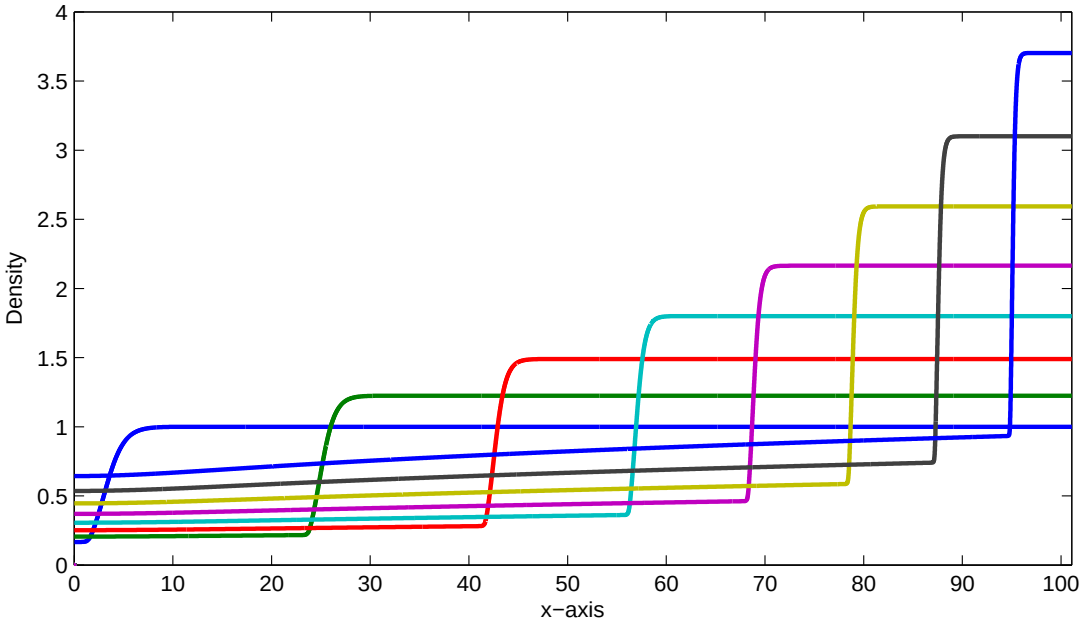

Figure 4.3: Density vs. $x - axis$ for $q = 5$ at consecutive time steps

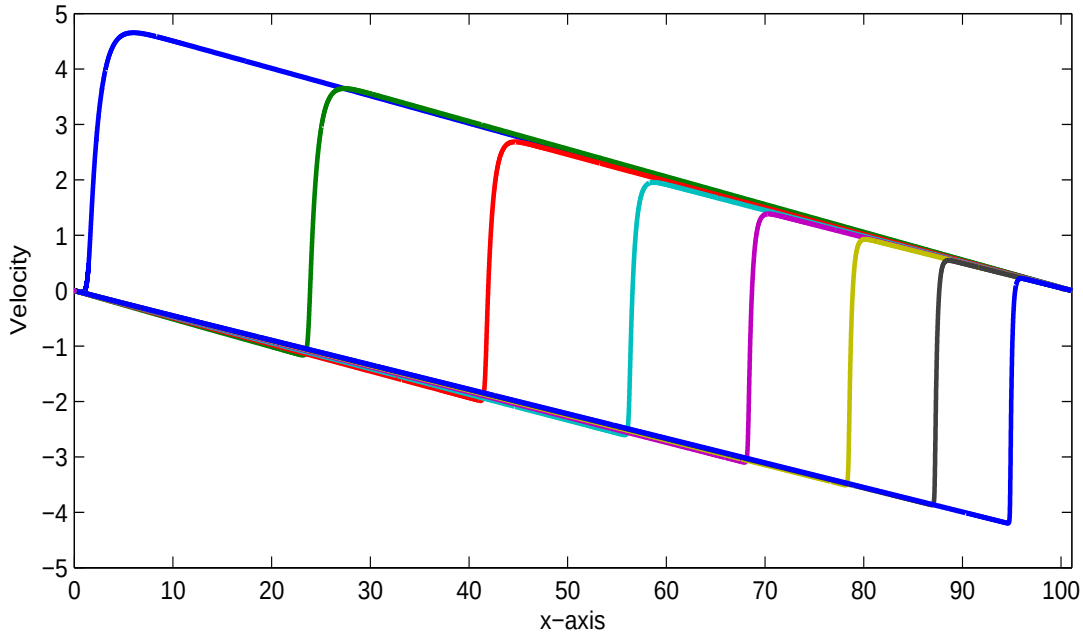

Figure 4.4: Velocity vs. $x - axis$ for $q = 5$ at consecutive time steps

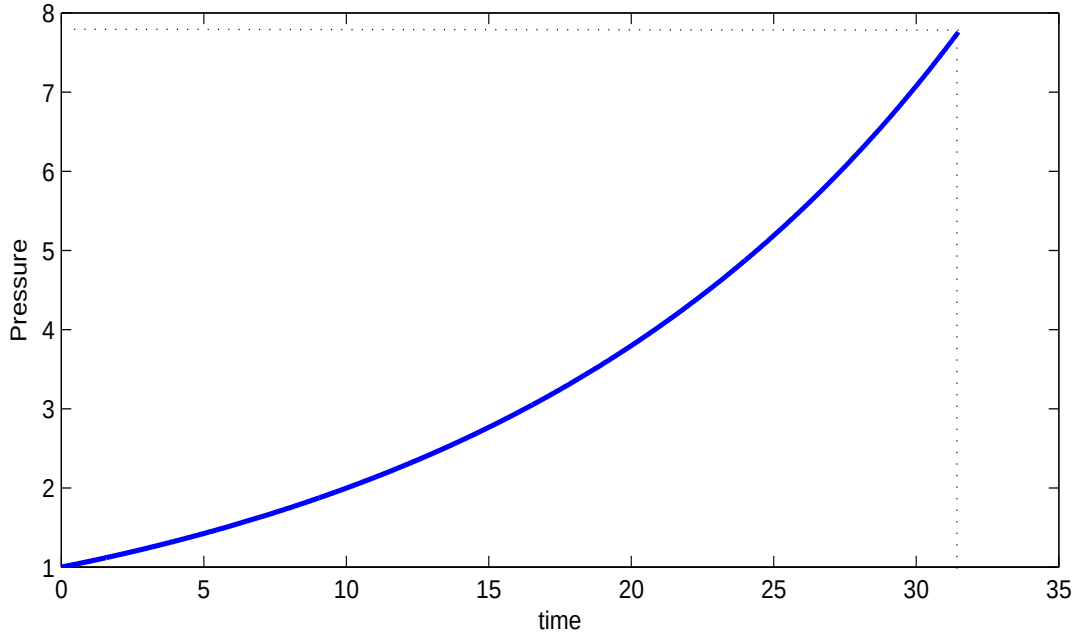

Figure 4.5: Pressure vs time

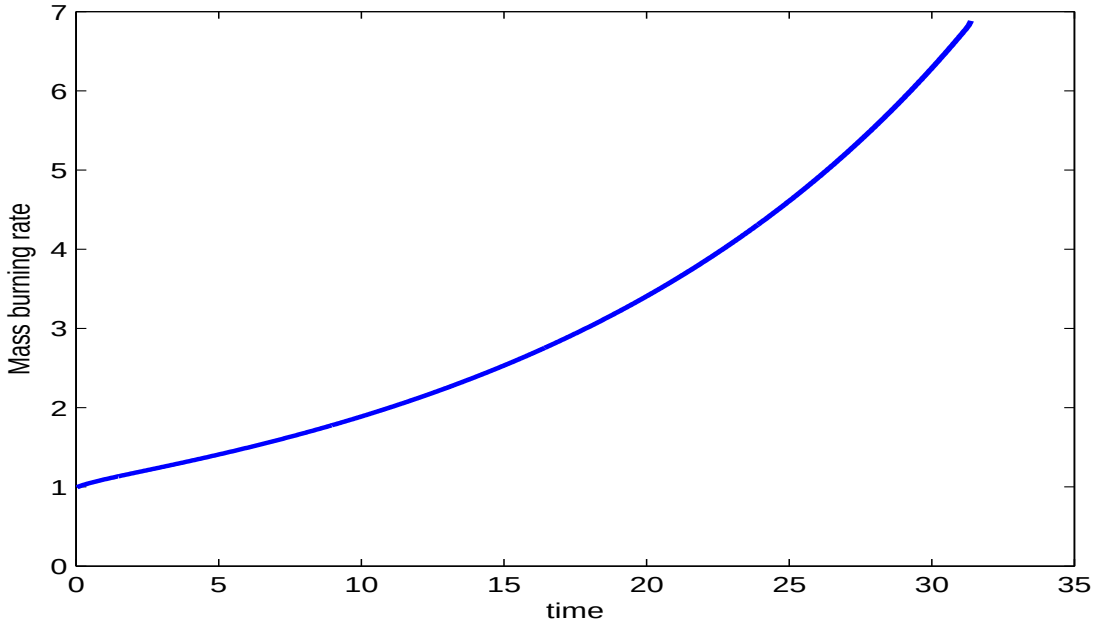

Figure 4.6: Mass burning rate vs. time

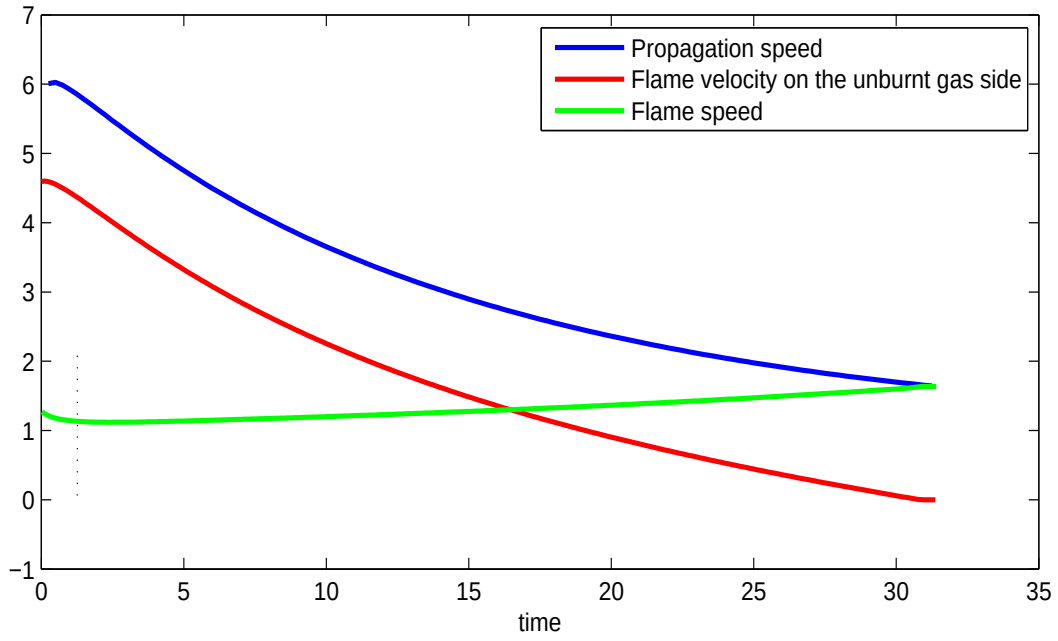

Figure 4.7: Propagation and flame speed vs. time

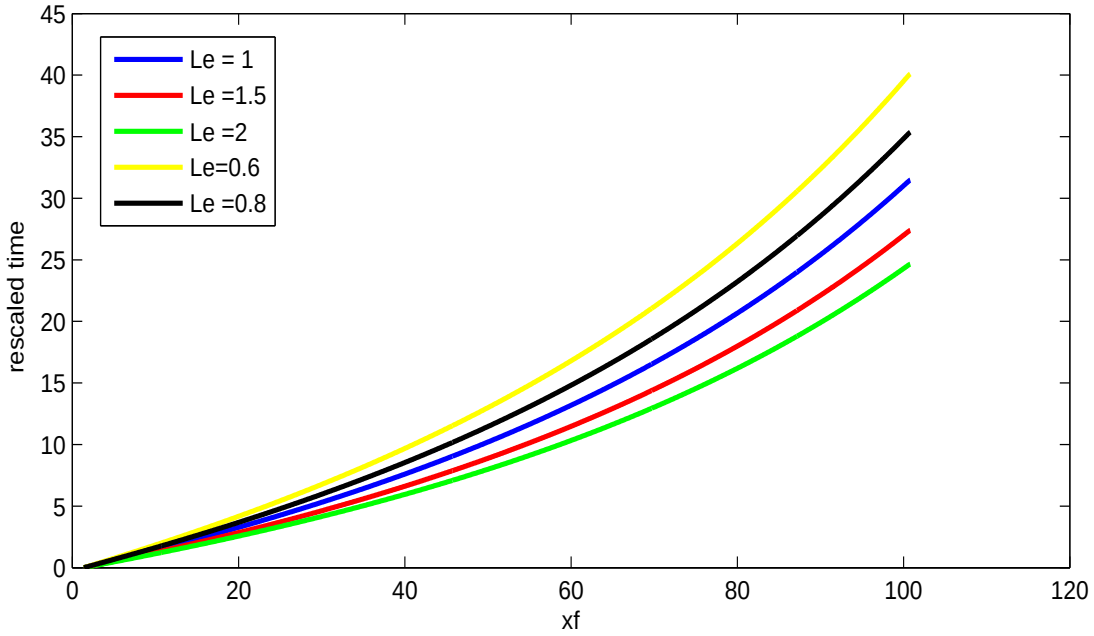

Figure 4.8: Rescaled time vs flame location as a function of Le number

The parameters for the plots are : $L = 100$, β=10, γ=1.4. In the temperature field plot (4.1), as the flame propagates from left to right, the flame thickness reduces as the pressure increases in the confined channel. The adiabatic compression also causes the temperature of the fresh mixture to increase with time. From the plot of the velocity field figure (4.4), the fresh mixture is compressed and pushed to the right whereas the burnt products are pushed away from the region of the flame towards the left end of the channel. There is a small error which is seen in the plot of the flame speed (4.7) because of the initial location of the flame which is not exactly at x=0. Also the flame has a definite thickness. This causes the non-dimensionalized flame speed to be not equal to 1 exactly at time $t = 0$. In the last plot(4.8), the effect of Lewis number on the time it takes for the flame to propagate the entire length of the channel is shown. The non-dimensionalization of t depends on Le and hence the time axis is rescaled such that $t^* = \frac{tS_{L_0}}{l_f}$, where S_{L_0} is the laminar flame speed for an unconfined planar flame under isobaric, adiabatic conditions for $Le = 1$.

4.2 Flame propagation in a confined channel - Analytical solution

In the general form of the governing equations mentioned before, it is found that the viscosity, thermal and mass diffusion terms and the reaction terms are of $O(\delta)$ where $\delta = \frac{l_f}{l} = \frac{1}{L} << 1$. The length of the flame l_f is very small compared to the length of the channel l.

4.2.1 Hydrodynamic model

The full form of the governing equations can be rescaled to see the similarity between the hydrodynamic model and the numerical solution described above. The rescaling is done as follows. Let the time be rescaled as $\hat{t} = \dfrac{t}{L}$ and the spatial coordinate as $\hat{x} = \dfrac{x}{L}$ where $\dfrac{1}{L} << 1$.

For the sake of simplicity the symbol $\hat{}$ is dropped from all the terms below.

By this rescaling factor, $0 \leq x \leq 1$.

The mass conservation equation becomes

$$\frac{\partial \rho}{\partial t} + \frac{\partial}{\partial x}(\rho u) = 0.$$

The energy conservation equation becomes

$$\rho \frac{\partial T}{\partial t} + \rho u \frac{\partial T}{\partial x} = \frac{1}{L}\frac{\partial^2 T}{\partial x^2} + \left(\frac{\gamma - 1}{\gamma}\right)\frac{dP}{dt} + qL\omega.$$

The equation for the fuel mass fraction is

$$\rho \frac{\partial Y}{\partial t} + \rho u \frac{\partial Y}{\partial x} = \frac{1}{L}\frac{1}{Le}\frac{\partial^2 Y}{\partial x^2} - L\omega.$$

The equation of state is

$$P(t) = \rho T.$$

Also we have (as derived in the numerical model),

$$\frac{\partial u}{\partial x} = \frac{1}{P}\left(\frac{-1}{\gamma}\frac{dP}{dt} + \frac{1}{L}\frac{\partial^2 T}{\partial x^2} + Lq\omega\right). \tag{4.3}$$

In the limit $L >> 1$ and away from the flame, where $\omega \approx 0$ the equations simplifies as follows

The mass conservation equation is

$$\frac{\partial \rho}{\partial t} + \frac{\partial}{\partial x}(\rho u) = 0.$$

The energy conservation equation becomes

$$\rho\frac{\partial T}{\partial t} + \rho u\frac{\partial T}{\partial x} = \left(\frac{\gamma - 1}{\gamma}\right)\frac{dP}{dt}.$$

The equation for the concentration of species becomes

$$\rho\frac{\partial Y}{\partial t} + \rho u\frac{\partial Y}{\partial x} = 0.$$

The equation of state is

$$P(t) = \rho T.$$

From (4.3) we also have,

$$\frac{\partial u}{\partial x} = \frac{1}{P}\left(\frac{-1}{\gamma}\frac{dP}{dt}\right). \tag{4.4}$$

Using the equation of state, the energy equation can be rewritten as

$$\rho\frac{\partial}{\partial t}(\frac{P}{\rho}) + \rho u\frac{\partial}{\partial x}(\frac{P}{\rho}) = \frac{\gamma - 1}{\gamma}\frac{dP}{dt}.$$

Since P is only a function of t, the above relation can be simplified as follows

$$\gamma \frac{P}{\rho} \frac{D\rho}{Dt} = \frac{DP}{Dt}.$$

This equation can be written as

$$\frac{D}{Dt}(\rho^{-1} P^{1/\gamma}) = 0. \tag{4.5}$$

Thus

$$\frac{Ds}{Dt} = 0, \tag{4.6}$$

where

$$s = \rho^{-1} P^{1/\gamma}$$

s is defined as the entropy function.

These equations need to be solved subject to the Rankine Hugoniot jump relations across the interface - the flame front. $\vec{n}$ is unit normal pointing forward towards the burnt gas i.e $\vec{n} = \hat{i}$ and the flame front is given by $F(x,t) = 0$, or explicitly by $x = x_f(t)$. The Rankine Hugoniot relations are:

$$[\rho(\vec{v}.\vec{n} - \dot{x_f})] = 0, \tag{4.7}$$

$$[\vec{v} \times \vec{n}] = 0, \tag{4.8}$$

$$[p + \rho(\vec{v}.\vec{n} - \dot{x_f})(\vec{v} \cdot \vec{n})] = 0, \tag{4.9}$$

$$[T] = q. \tag{4.10}$$

where [ ] denotes the jump in the value, i.e burnt side minus the unburnt side.

Recall that the relation for pressure rise with time was derived as

$$\frac{dP}{dt} = \frac{\gamma q}{V} \int \omega dV,$$

where V is the volume of the vessel. When the flame shrinks to a surface this relation is also equal to

$$\frac{dP}{dt} = \frac{\gamma q}{V} \lim_{\Delta n \to 0} \int_{\Delta n} \int_{surface} \omega' \delta(n) dS dn,$$

where δ is the Dirac δ function and n is measured along the normal to the flame surface and ω' is the surface reaction rate such that $\omega' = \omega'(t)$.

Thus the pressure rise can be determined from

$$\frac{dP}{dt} = \frac{\gamma q}{V} \int \omega' dS.$$

Integration of the equation for fuel mass fraction across the flame surface (similar to the derivation of the Rankine Hugoniot relations) gives

$$[\rho(v \cdot n - \dot{x_f})Y] = -\omega',$$

which can be further rewritten as

$$M[Y] = \omega',$$

such that

$$\omega' = M.$$

The relation for pressure rise in the channel becomes

$$\frac{dP}{dt} = \gamma q M.$$

The dependence of the mass burning rate (M) on pressure and flame temperature is asssumed of the form

$$M = P^{1/2} \left(\frac{T_f}{T_a} \right)^{\frac{3}{2}} e^{\left(\frac{\beta_0}{2} \left(\frac{1}{T_a} - \frac{1}{T_f} \right) \right)}, \tag{4.11}$$

which is a generalization of the analytical expression derived for unconfined planar flames (see section 4.2.7), where T_f is the flame temperature. Here β_0 is the activation energy parameter given by $\beta_0 = \dfrac{E}{RT_0}$. We note that a relation between β and β_0 is $\beta_0 = \beta \dfrac{(q+1)^2}{q}$. The Euler equations are now solved analytically in order to obtain the solution of the variables like pressure, velocity, temperature and density in the unburnt and burnt side of the gas.

4.2.2 Boundary Conditions

The boundary conditions along the walls of the channel are

$$\frac{\partial T}{\partial x} = \frac{\partial Y}{\partial x} = 0. \tag{4.12}$$

4.2.3 Summary of the governing equations for the Hydrodynamic model

The mathematical problem involves solving the following time dependent one -dimensional equations.

$$\frac{\partial u}{\partial x} = -\frac{1}{\gamma P} \frac{dP}{dt},$$

$$P = \rho T,$$

$$Ds/Dt = 0 \text{ where } s = \rho^{-1} P^{\frac{1}{\gamma}},$$

$$dP/dt = \gamma q M,$$

where

$$M = P^{1/2} \left(\frac{T_f}{T_a} \right)^{\frac{3}{2}} e^{\left(\frac{\beta_0}{2} \left(\frac{1}{T_a} - \frac{1}{T_f} \right) \right)}.$$

Across $x = x_f(t)$:

$$[\rho(u - \dot{x_f})] = 0, \tag{4.13}$$

$$[p + \rho u(u - \dot{x_f})] = 0, \tag{4.14}$$

$$[T] = q. \tag{4.15}$$

4.2.4 Analytical solution to the 1-D planar flame

This part discusses the **analytical solution** to the 1-D planar flame problem to compute the value of properties like pressure, temperature, velocity and density.

Velocity for burnt and unburnt gas:

For the burnt gas the following boundary condition is applicable.

At $x = 0, u = 0$ (Boundary condition at the wall)

Integrating (4.4) w.r.t the variable x and applying the above boundary condition, we get

$$u_b = -\frac{\dot{p}}{\gamma P}x. \tag{4.16}$$

For the case of unburnt gases the following boundary condition is applicable.

At $x = 1, u = 0$ (Boundary condition at the wall) Integrating (4.4) wrt the variable x and applying the above boundary condition, we get

$$u_u = \frac{\dot{p}}{\gamma P}(1 - x). \tag{4.17}$$

Thus,

$$u(x,t) = \begin{cases} -\dfrac{\dot{p}}{\gamma P}x & \text{if } x < x_f, \\ \dfrac{\dot{p}}{\gamma P}(1-x) & \text{if } x > x_f. \end{cases}$$

Density and temperature for unburnt gas:

From equation (4.6) we have

$$\frac{Ds}{Dt} = 0$$

or s is a constant along a streamline.

$$s = \rho^{-1} P^{\frac{1}{\gamma}}.$$

We have the initial conditions $P = P_0$ and $\rho = \rho_0$.

Thus we get

$$\rho^{-1} P^{\frac{1}{\gamma}} = 1.$$

The density of the unburnt gas is

$$\rho_u = P^{\frac{1}{\gamma}} \tag{4.18}$$

and the temperature of the unburnt gas is

$$T_u = \frac{P}{\rho} = P^{\frac{\gamma-1}{\gamma}}. \tag{4.19}$$

Temperature and density at x_f-, at the flame in the burnt gas side:

Using the temperature jump relation, the temperature at the flame on the burnt side at x_f- is

$$T_f\text{-} = P^{\frac{\gamma-1}{\gamma}} + q \tag{4.20}$$

and the density at the flame on the burnt side at x_f- is

$$\rho_{f^-} = \frac{P}{T_{f^-}} = \frac{P}{P^{\frac{\gamma-1}{\gamma}} + q}. \tag{4.21}$$

Applying the jump relation as mentioned in (4.13), we have

$$\rho(u - \dot{x_f})]_{x_f-} = \rho(u - \dot{x_f})]_{x_f+}. \tag{4.22}$$

Substituting the obtained expressions from equations (4.16), (4.17), (4.18) and (4.21) into (4.22), we get

$$\frac{P}{P^{\frac{\gamma-1}{\gamma}} + q}(-\frac{1}{\gamma}\frac{\dot{P}}{P}x_f - \dot{x_f}) = P^{\frac{1}{\gamma}}(\frac{1}{\gamma}\frac{\dot{P}}{P}(1 - x_f) - \dot{x_f})$$

which is simplified as

$$\frac{d}{dt}(-PL + \gamma q(P^{\frac{1}{\gamma}}(x_f - 1))) = 0$$

or

$$(-PL + \gamma q(P^{\frac{1}{\gamma}}(x_f - 1))) = \text{constant} = \text{C(say)}. \tag{4.23}$$

Applying the initial condition, at $t = 0$ we have $P = 1$ and x_f =0.

$$1 + \gamma q = -C$$

Also at x_f =1, P = P_e, which gives

$$-P_e = C$$

. Thus we get the **end pressure** in the confined channel P_e as

$$P_e = 1 + \gamma q = -C = \text{constant}. \tag{4.24}$$

Combining equations (4.23) and (4.24), we get a relation for the **position of the flame** as a function of the pressure P and the end pressure P_e as follows,

$$x_f = 1 - (\frac{P_e - P}{P_e - 1})P^{\frac{1}{\gamma}}. \tag{4.25}$$

Temperature and density distribution in burnt gas

From equation (4.6) we have

$$\frac{Ds}{Dt} = 0,$$

that is

$$\frac{\partial s}{\partial t} + u\frac{\partial s}{\partial x} = 0,$$

where

$$s = TP^{\frac{1-\gamma}{\gamma}}.$$

Substituting (4.17) in the above equation, we get

$$\frac{\partial s}{\partial t} - \frac{1}{\gamma}\frac{\dot{P}}{P}x\frac{\partial s}{\partial x} = 0.$$

The general solution to this equation is given by

$$s = \psi(xP^{\frac{1}{\gamma}}),$$

where the functional form of ψ remains to be determined.

From (4.20), we have

$$T_f = P^{\frac{1-\gamma}{\gamma}} + q.$$

Thus

$$T_f P^{\frac{1-\gamma}{\gamma}} = 1 + qP^{\frac{1-\gamma}{\gamma}},$$

$$s_f = 1 + qP^{\frac{1-\gamma}{\gamma}}.$$

Thus we get

$$\psi(x_f P^{\frac{1}{\gamma}}) = 1 + qP^{\frac{1-\gamma}{\gamma}}.$$

Substituting the value of x_f as obtained from (4.25), we get

$$\psi\left(P^{\frac{1}{\gamma}} - \frac{P_e - P}{P_e - 1}\right) = 1 + qP^{\frac{1-\gamma}{\gamma}}.$$

Thus

$$\psi(\eta) = 1 + qP^{\frac{1-\gamma}{\gamma}},$$

where

$$\eta = (P^{\frac{1}{\gamma}} - \frac{P_e - P}{P_e - 1}).$$

As the pressure as a function of time is known, by plotting the above function for different values of η, the density and the temperature in the burnt side of the gas can be found.

Thus,

$$T(x,t) = \begin{cases} P^{\frac{\gamma-1}{\gamma}} & \text{if } x > x_f, \\ P^{\frac{(\gamma-1)}{\gamma}} s(x,t) & \text{if } x < x_f. \end{cases}$$

$$\rho(x,t) = \begin{cases} P^{\frac{1}{\gamma}} & \text{if } x > x_f, \\ \dfrac{P^{\frac{1}{\gamma}}}{s(x,t)} & \text{if } x < x_f. \end{cases}$$

4.2.5 Results and plots

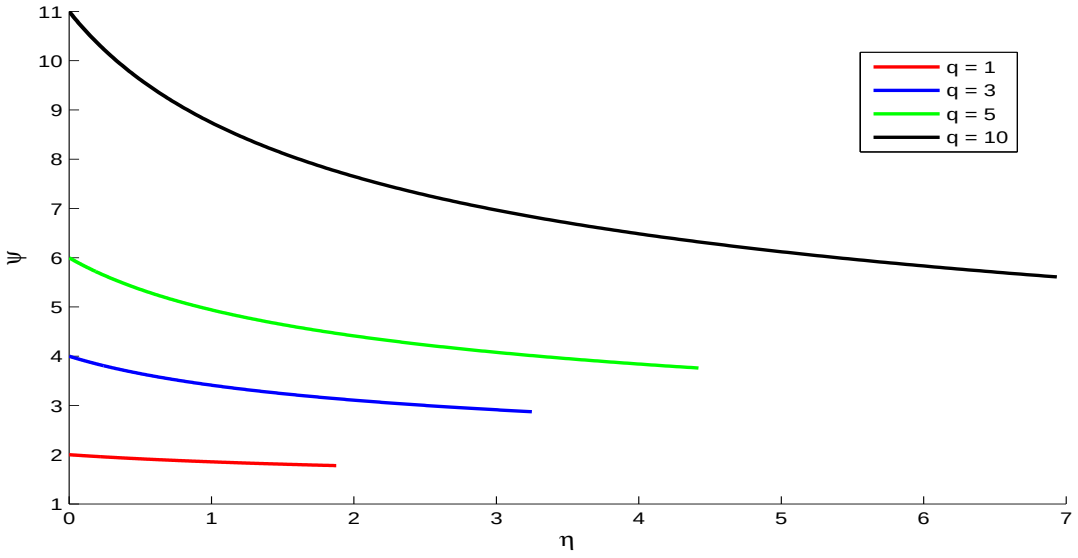

Figure 4.9: ψ vs. η for $q = 1$, 3, 5 and 10

4.2.6 Comparison of the numerical and the analytical solution

The pressure in the channel when the flame is at the end of the channel should ideally be $P_e = 1 + \gamma q$ as derived for the hydrodynamic model, but this value differs with the plot of the numerical solution (4.5) as the flame is assumed to have an initial thickness and its initial location is at a small distance away from the left end of the channel and not exactly at $x = 0$.

We compare the plots of the mass buring rate that were obtained from the numerical and the analytical solution. (Figures 4.17, 4.16 are shown for $Le = 1$ and $q = 5$). The parameters for the numerical model have been rescaled to those of the hydrodynamic model so that the plots for the numerical solution and analytical solution can be plotted on the same graph. These plots show that the plots obtained by the numerical solution agree very well with those of the analytical solution.

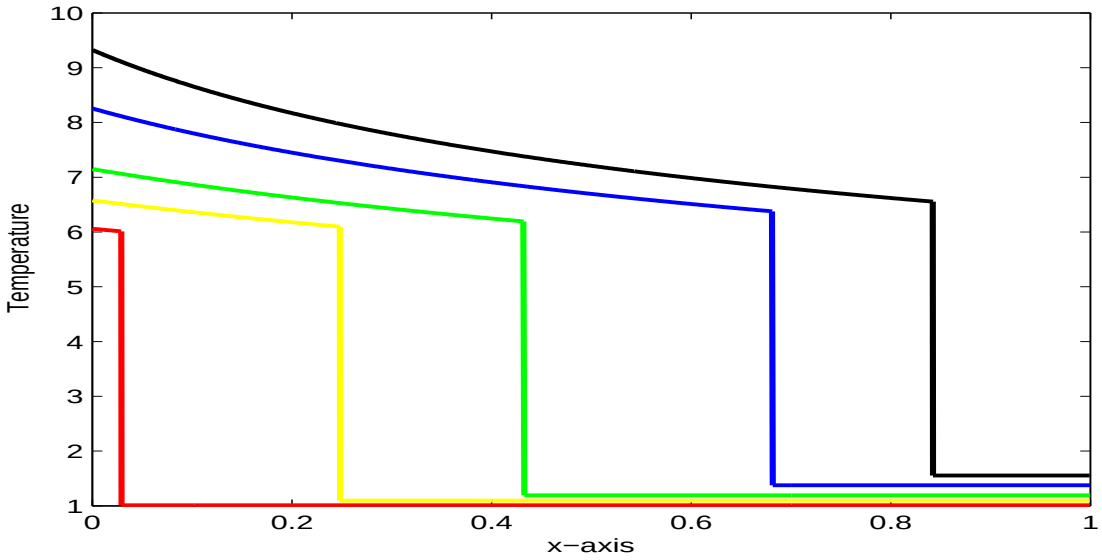

Figure 4.10: Temperature vs. $x - axis$ for time t =0.005, 0.05, 0.1, 0.2 and 0.3, $q = 5$

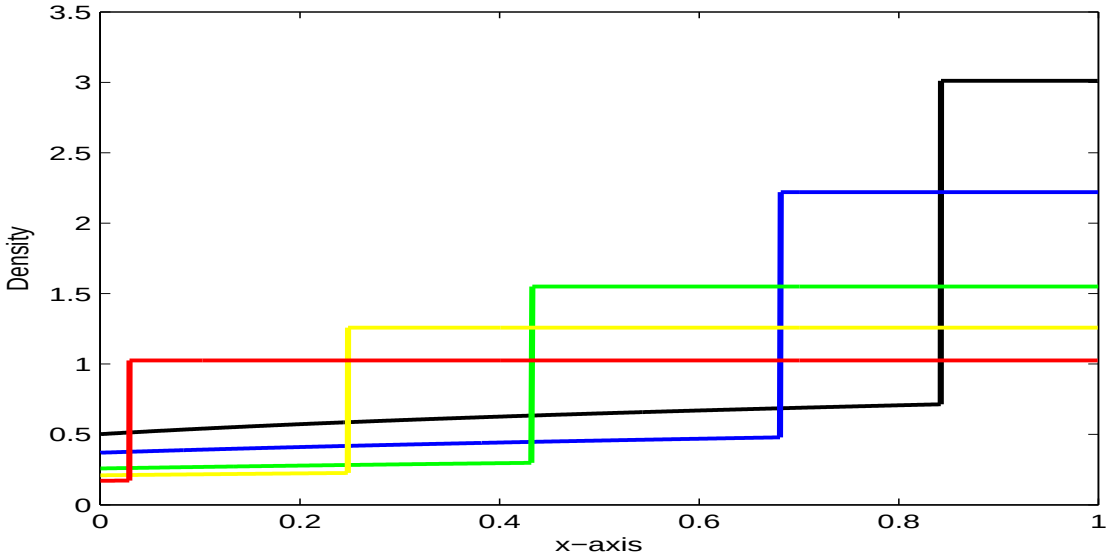

Figure 4.11: Density vs. $x - axis$ for time t =0.005, 0.05, 0.1, 0.2 and 0.3, $q = 5$

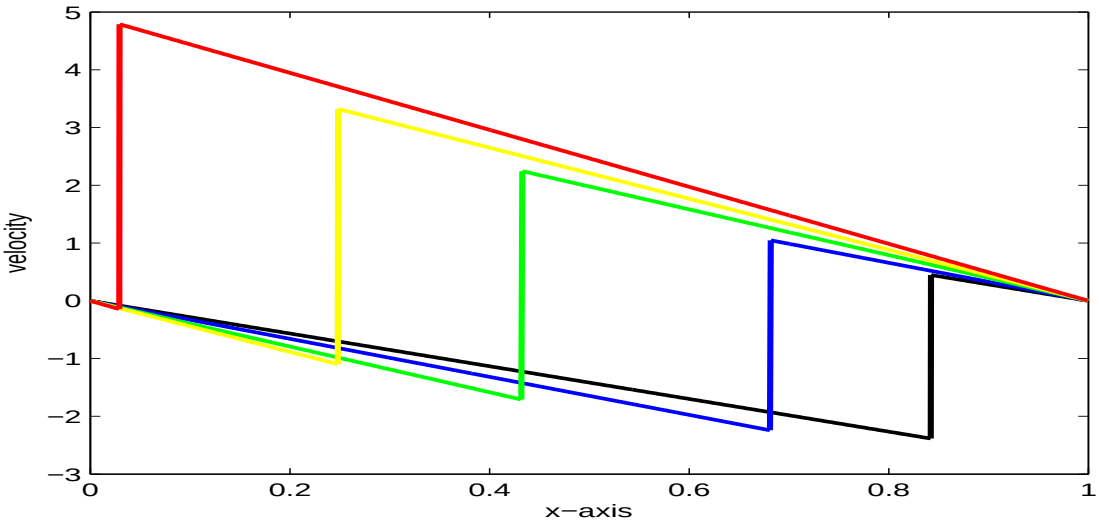

Figure 4.12: Velocity field vs. $x - axis$ for time t =0.005, 0.05, 0.1, 0.2 and 0.3, $q = 5$

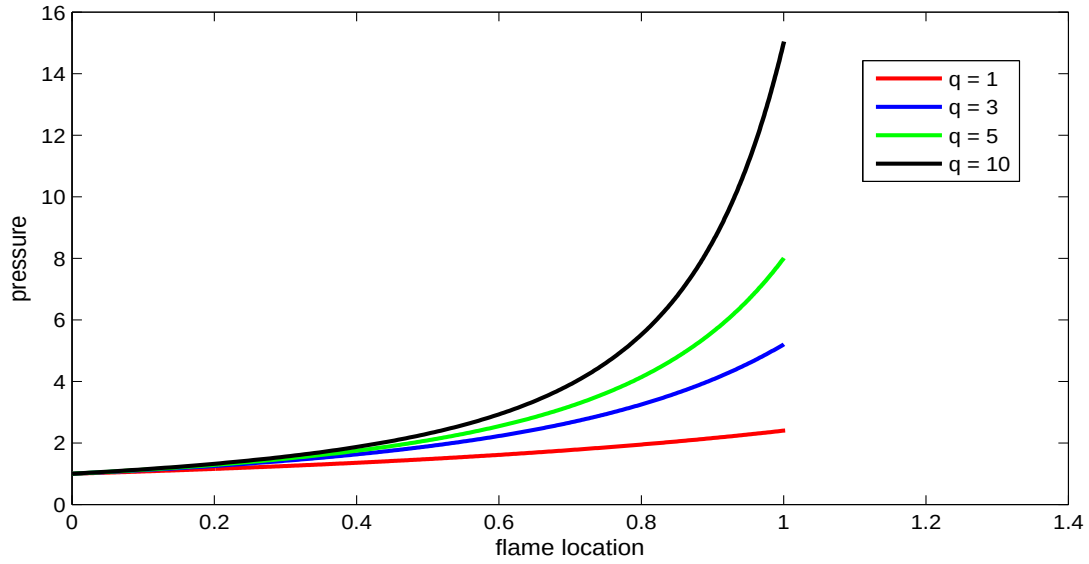

Figure 4.13: Pressure vs. location of flame for $q = 1$, 3, 5 and 10

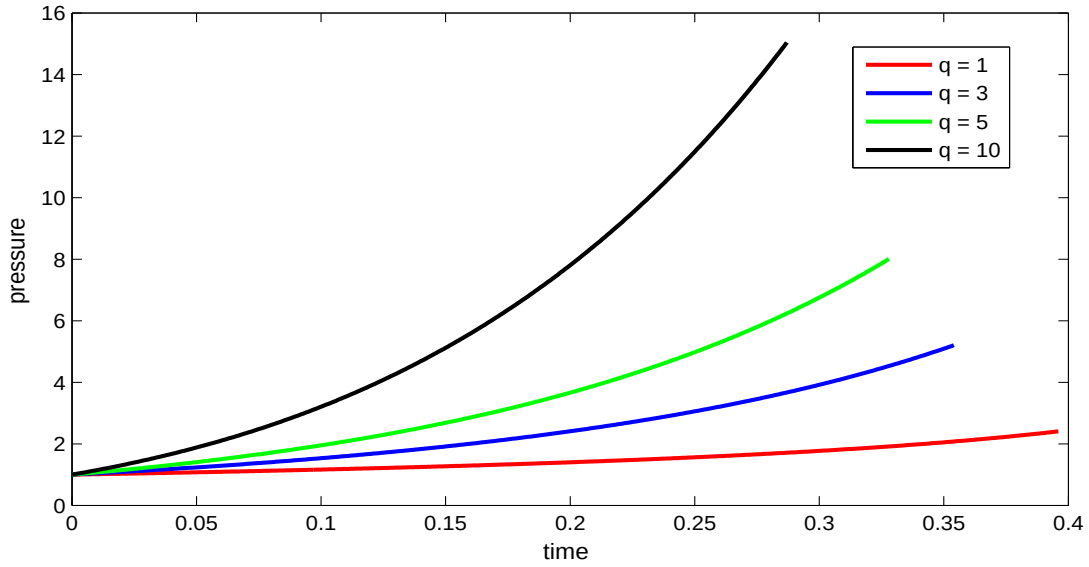

Figure 4.14: Pressure vs. time for $q = 1$, 3, 5 and 10

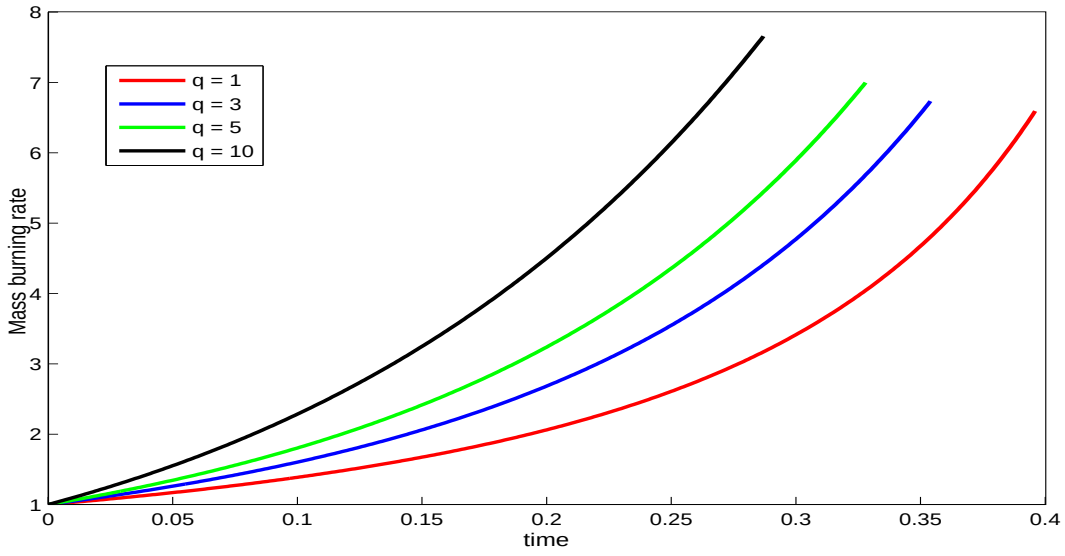

Figure 4.15: Mass burning rate vs. time for $q = 1$, 3, 5 and 10

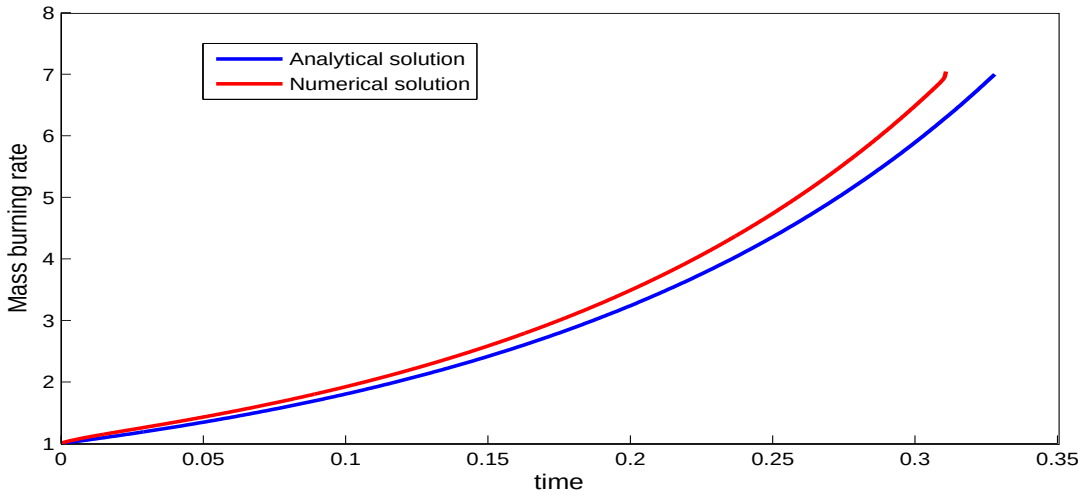

Figure 4.16: Mass burning rate vs. time comparison for the numerical model and Hydrodynamic model

4.2.7 Expression for mass burning rate

In the dimensional form (* is not written for convenience), the burning rate of an unconfined adiabatic planar flame is given by

$$M_0 = \rho_u S_L = \sqrt{\frac{2\rho_b(\lambda/c_p)B}{\beta^2 Le^{-1}}}\, e^{-E/2RT_a},$$

where

$$\beta = \frac{E}{RT_a{}^2}(T_a - T_0) = \frac{E}{RT_a{}^2}\frac{QY_0}{c_p}.$$

We make the proposition that the burning rate (M) of a confined adiabatic flame takes the form similar to the above expression (M_0) but the burning rate (M) now depends on the flame temperature T_f instead of the the adiabatic flame temperature T_a.

$$M = \rho_u S_L = \sqrt{\frac{2\rho_f(\lambda/c_p)B}{\beta_{new}{}^2 Le^{-1}}}\, e^{-E/2RT_f},$$

where β_{new} is the Zel'dovich parameter for the confined case. We also have the equation of state $P(t) = \dfrac{\rho_f RT_f}{W}$ for the confined case and $P_0 = \dfrac{\rho_b RT_a}{W}$ for the unconfined case where P_0 is the atmospheric pressure.

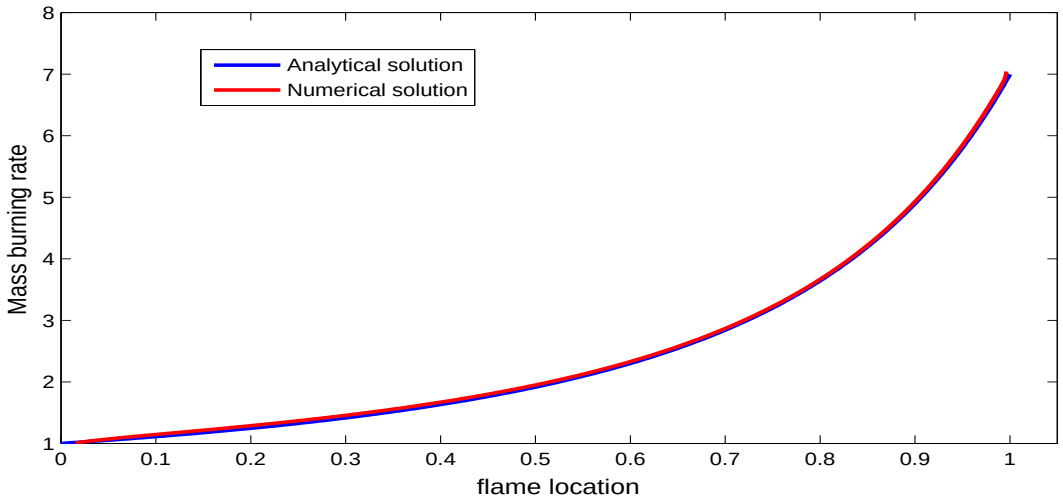

Figure 4.17: Mass burning rate vs. location of flame comparison for the numerical model and Hydrodynamic model

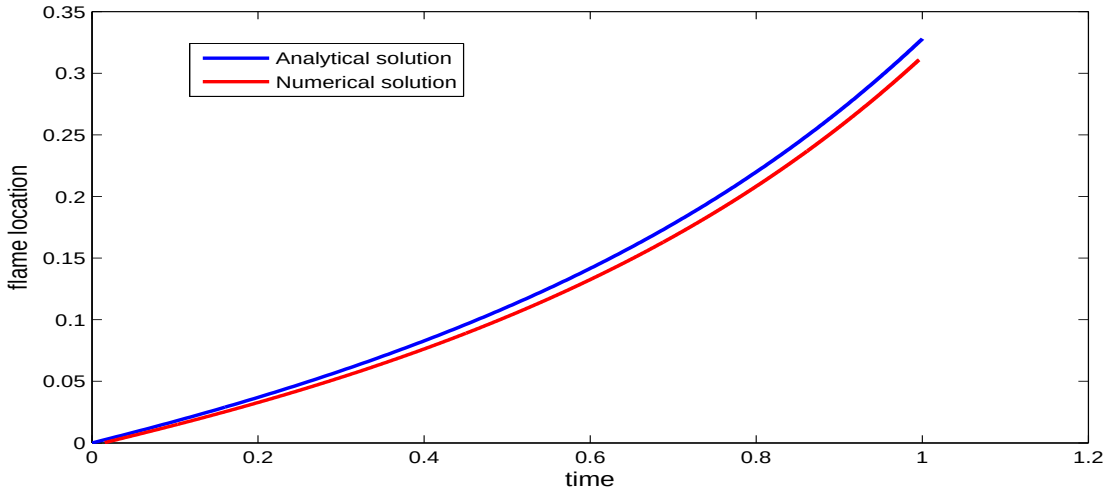

Figure 4.18: Location of flame vs. time comparison for the numerical model and Hydrodynamic model

Two different cases for β_{new} can be argued.

Case 1: β_{new} doesn't depend on the local flame temperature, i.e $\beta_{new} = \beta$:

If β_{new} doesn't depend on the local flame temperature, then mass burning rate can be written as

$$M = \left(\frac{P}{P_0}\right)^{\frac{1}{2}} \left(\frac{T_f}{T_a}\right)^{-\frac{1}{2}} e^{\left(\frac{E}{2RT_a} - \frac{E}{2RT_f}\right)} M_0. \tag{4.26}$$

If we non-dimensionalize equation (4.26) as outlined in chapter 2, we get an expression for the mass burning rate in a confined channel as,

$$M = P^{\frac{1}{2}} \left(\frac{T_f}{T_a}\right)^{-\frac{1}{2}} e^{\left(\frac{\beta_0}{2}\left(\frac{1}{T_a} - \frac{1}{T_f}\right)\right)}, \tag{4.27}$$

where $\beta_0 = E/RT_0$.

Case 2: β_{new} depends on the local flame temperature:

If β_{new} depends on the local flame temperature, we can write

$$\beta_{new} = \beta \left(\frac{T_a}{T_f}\right)^2$$

, then mass burning rate in the dimensional form can be written as

$$M = \left(\frac{P}{P_0}\right)^{\frac{1}{2}} \left(\frac{T_f}{T_a}\right)^{\frac{3}{2}} e^{\left(\frac{E}{2RT_a} - \frac{E}{2RT_f}\right)} M_0. \tag{4.28}$$

If we non-dimensionalize equation (4.28), we get an expression for the mass burning rate in a confined channel as,

$$M = P^{\frac{1}{2}} \left(\frac{T_f}{T_a}\right)^{\frac{3}{2}} e^{\left(\frac{\beta_0}{2}\left(\frac{1}{T_a} - \frac{1}{T_f}\right)\right)}. \tag{4.29}$$

We compare equations (4.27) and (4.29) with the obtained numerical solution to determine which expression represent the mass buring rate in a confined channel. From the plots (4.19)

and (4.20), it is seen that the mass burning rate given by equation (4.29) agrees well with that of the mass burning rate computed numerically. Equation (4.29) has therefore been used in this thesis as the expression to the mass buring rate in the the hydrodynamic model; see equation (4.11).

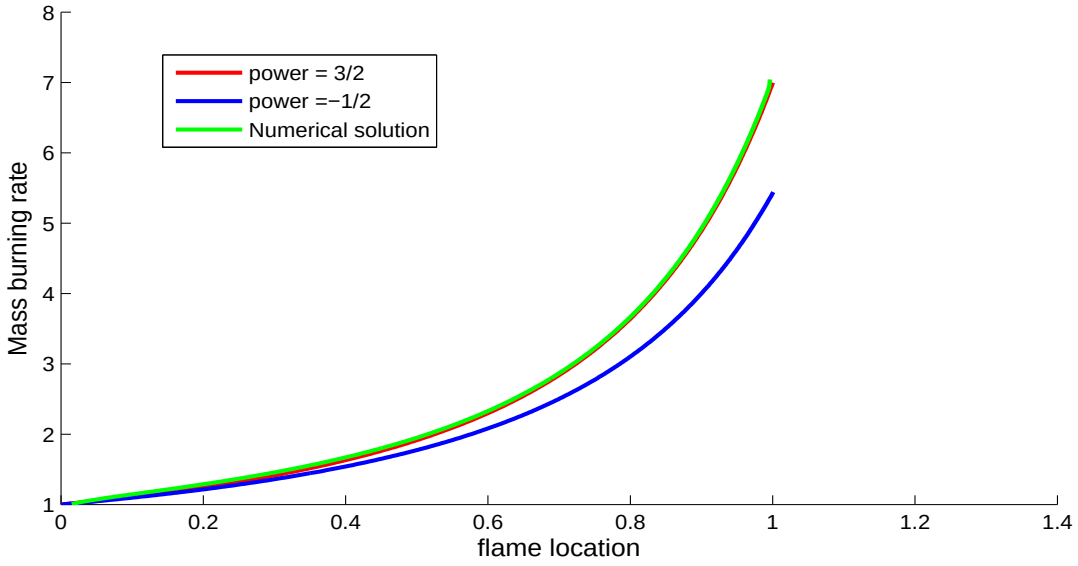

Figure 4.19: Comparison of the analytical expression of mass burning rate with the numerically obtained mass burning rate: Mass burning rate vs. flame location

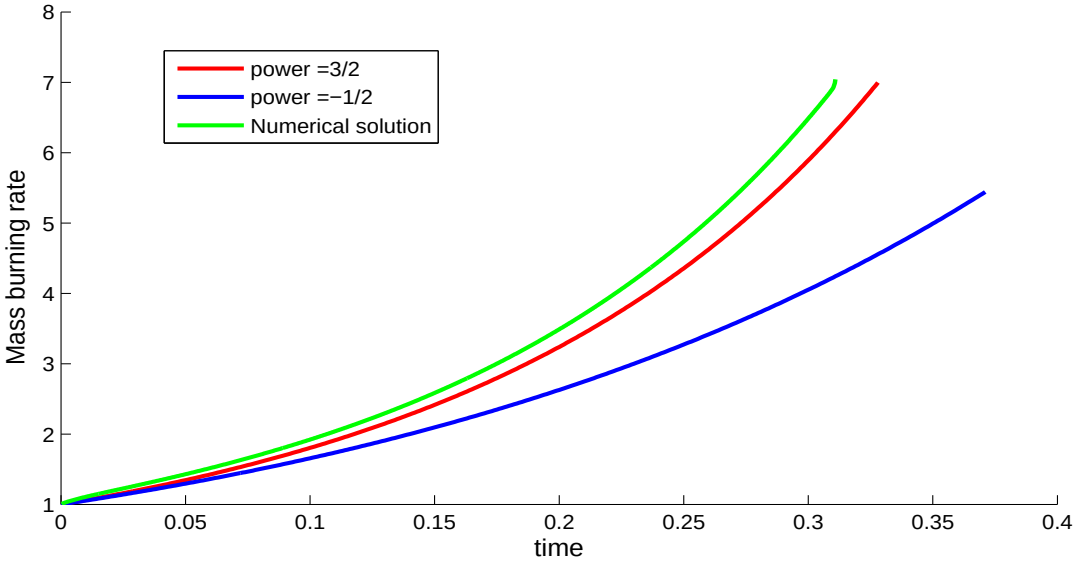

Figure 4.20: Comparison of the analytical expression of mass burning rate with the numerically obtained mass burning rate: Mass burning rate vs. time

Chapter 5

Conclusion

For the case of premixed flames in unconfined channels, the steady state solution to the planar flame problem was studied numerically. The structure of the flame and the flame speed parameter s_L (which is directly related to the flame speed) were obtained numerically for various values of the Lewis number and the Zel'dovich number. The time dependent problem was also studied showing that indeed the flame propagates steadily at a constant speed. The plot of flame location vs. time is a straight line with a slope that agrees well with the results obtained by solving the steady equations.

For the case of premixed flames in confined channels, the problem is intrinsically unsteady. As a result of confinement there is pressure buildup and the flame accelerates as it moves from one end of the channel to the other end. This problem was addressed in two different ways:

The first is a hydrodynamic model where the entire flame is treated as a surface and flow field solved subject to the Hugoniot jump conditions across the flame. The reaction rate is therefore considered as a delta - function with a strength suggested by the asymptotic solutions of unconfined flames. Analytical expressions for the location of the flame sheet , flame temperature as a function of time have been obtained.

The second approach is a numerical solution of the complete governing equations that correspond therefore to finite rate chemistry. The pressure, propagation speed, flame speed, gas velocity as well as the temperature and density profiles agree well with the solution to the Hydrodynamic model. Further the numerical solution gives an insight into the thickness of the flame as it varies through the channel. It is seen that with the pressure build-up in the

channel, the thickness of the flames reduces as the reaction zone becomes becomes thinner due to significant increase in temperature.

It should be noted that the mass burning rate that was calculated numerically, matches with the analytical solution presented in the hydrodynamic model extremely well, suggesting that treating the flame as a discontinuity with the proposed delta-function expression for the reaction rate represents a good approximation to the problem.

Chapter 6

References

[1] W. B. Bush and F. E. Fendell, "Asymptotic analysis of laminar flame propagation for general lewis numbers," *Combustion Science and Technology*, vol. 1, pp. 421–428, 1970.

[2] F. E. Fendell, "Asymptotic analysis of premixed burning with large activation energy," *Journal of Fluid Mechanics*, vol. 56:part 1, pp. 81–95, 1972.

[3] Y. B. Zeldovich, G.I.Barrenblatt, V. B. Librovich, and G. M. Makhviladze, *The Mathematical Theory of Combustion and Explosions*. 1980.

[4] J. D. Buckmaster and J. S. S. Ludford, *Lectures on Mathematical Combustion*. SIAM, Philadelphia, 1983.

[5] F. A. Williams, *Combustion Theory*. Perseus Books Publishing, 1985.

[6] M. Matalon and B.J.Matkowsky, "Flames as gasdynamic discontinuities," *Journal of Fluid Mechanics*, vol. 124, pp. 239–259, 1982.

[7] C. Cui, M. Matalon, J. Daou, and J. Dold, "Effect of differential diffusion on thin and thick flames propagating in channels," *Combustion Theory and Modelling, 8*, pp. 41–64, 2004.

[8] F. Benkhaldoun, B. Larrouturou, and B. Denet, "Numerical investigation of the extinction limit of curved flames," *Combustion Science and Technology*, vol. 64, pp. 187–198, 1989.

[9] J. Daou and M. Matalon, "Flame propagation in poiseuille flow under adiabatic conditions," *Combustion and Flame*, vol. 124, pp. 337–349, 2001.

[10] J. Daou and M. Matalon, "Influence of conductive heat-losses on the propagation of premixed flames in channels," *Combustion and Flame*, vol. 128, pp. 321–339, 2002.

[11] V. Kurdyumov and M. Matalon, "The propagation of premixed flames in closed tubes," *Proceedings of the Combustion Institute*. In press.

[12] D. Bradley and A. Mitcheson, "Mathematical solutions for explosions in spherical vessels," *Combustion and Flame*, vol. 26, pp. 201–217, 1976.

[13] G.I.Sivashinsky, "Hydrodynamic theory of flame propagation in an enclosed volume," *Acta Astronautica*, vol. 6, pp. 631–645, 1979.

[14] D. E.Cooker, "Transient laminar flame propagation in confined premixed gases: Numerical predictions," *Symposium (International) on Combustion*, vol. 17, no. 1, pp. 1329 – 1339, 1979. Seventeenth Symposium on Combustion.

[15] D. E.Cooker, "Numerical study of a confined premixed laminar flame: Oscillatory propagation and wall quenching," *Combustion and Flame*, vol. 49, pp. 141–149, 1983.

[16] S. F. Fink, F. E. Fendell, and W. B. Bush, "Nonadiabatic propagation of a planar premixed flame: Constant-volume enclosure," *AIAA Journal*, vol. 23, no. 3, pp. 424 – 431, 1985.

[17] J. L. Mcgreevy and M. Matalon, "Lewis number effect on the propogation of premixed flames in closed tubes," *Combustion and Flame*, vol. 91, pp. 213–225, 1992.

[18] M. Matalon and P. Metzener, "The propagation of premixed flames in closed tubes," *Journal of Fluid Mechanics*, vol. 336, pp. 331–350, 1997.

[19] F. Marra and G. Continillo, "Numerical study of premixed laminar flame propagation in a closed tube with a full navier-stokes approach," *Symposium (International) on Combustion*, pp. 907 – 913, 1996. Twenty-Sixth Symposium on Combustion.

[20] K. Kuzuu, K. Ishii, and K. Kuwahara, "Numerical simulation of of premixed flame propagation in a closed tube," *Elsevier*, vol. 18, pp. 165–182, 1996.

[21] D. G. Lasseigne, T. L. Jackson, and L. Jameson, "Stability of freely propagating flames revisited," *Combustion Theory and Modelling*, vol. 3:4, pp. 591–611, 1999.